Biomaterials 306 (2024) 122482

Contents lists available at ScienceDirect

Biomaterials

journal homepage: www.elsevier.com/locate/biomaterials

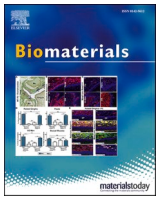

# On-chip recapitulation of the tumor microenvironment: A decade of progress

S.M. Giannitelli [a,1], V. Peluzzi [b,1], S. Raniolo [a], G. Roscilli [c], M. Trombetta [a], P. Mozetic [d], A. Rainer [b,e,*]

[a] Department of Science and Technology for Sustainable Development and One Health, Università Campus Bio-Medico di Roma, via Álvaro del Portillo, 21, 00128, Rome, Italy
[b] Department of Engineering, Università Campus Bio-Medico di Roma, via Álvaro del Portillo 21, 00128, Rome, Italy
[c] Takis s.r.l., Via di Castel Romano 100, 00128, Rome, Italy
[d] Institute of Nanotechnology (NANOTEC), National Research Council, via Monteroni, 73100, Lecce, Italy
[e] Fondazione Policlinico Universitario Campus Bio-Medico di Roma, via Álvaro del Portillo 200, 00128, Rome, Italy

ARTICLE INFO

*Keywords:*
Tumor microenvironment
Organ-on-a-chip
In vitro models
Tumor spheroids
Vascularization

ABSTRACT

One of the hurdles to the development of new anticancer therapies is the lack of *in vitro* models which faithfully reproduce the *in vivo* tumor microenvironment (TME). Understanding the dynamic relationships between the components of the TME in a controllable, scalable, and reliable setting would indeed support the discovery of biological targets impacting cancer diagnosis and therapy.

Cancer research is increasingly shifting from traditional two-dimensional (2D) cell culture toward three-dimensional (3D) culture models, which have been demonstrated to increase the significance and predictive value of *in vitro* data. In this scenario, microphysiological systems (also known as organs-on-chip) have emerged as a relevant technological platform enabling more predictive investigation of cell-cell and cell-ECM interplay in cancer, attracting a significant research effort in the last years.

This review illustrates one decade of progress in the field of tumor-microenvironment-on-chip (TMOC) approaches, exploiting either cell-laden microfluidic chambers or microfluidic confined tumor spheroids to model the TME. TMOCs have been designed to recapitulate several aspects of the TME, including tumor cells, the tumor-associated stroma, the immune system, and the vascular component. Significantly, the last aspect has emerged for its pivotal role in orchestrating cellular interactions and modulating drug pharmacokinetics on-chip. A further advancement has been represented by integration of TMOCs into multi-organ microphysiological systems, with the final aim to follow the metastatic cascade to target organs and to study the effects of chemotherapies at a systemic level.

We highlight that the increased degree of complexity achieved by the most advanced TMOC models has enabled scientists to shed new light on the role of microenvironmental factors in tumor progression, metastatic cascade, and response to drugs.

## 1. Introduction

The development of new cancer therapies has been hampered by the limitations of current non-clinical models to identify key molecular, cellular, and biophysical features of human cancer [1]. Although murine models enable the validation of treatments efficacy, they do not succeed in recapitulating the human tumor microenvironment (TME), which is critical for controlling cancer growth and progression [1].

The tumor microenvironment is a complex three-dimensional structure characterized by an altered and vascularized extracellular matrix (ECM) containing cancerous cells surrounded by different non-tumor cell types [2]. In particular, the non-tumoral component of TME consists of several cell types, including cancer-associated fibroblasts (CAFs), endothelial cells (ECs), immune cells (macrophages and

* Corresponding author. Department of Engineering, Università Campus Bio-Medico di Roma, via Álvaro del Portillo 21, 00128, Rome, Italy.
*E-mail addresses:* s.giannitelli@unicampus.it (S.M. Giannitelli), v.peluzzi@unicampus.it (V. Peluzzi), s.raniolo@unicampus.it (S. Raniolo), roscilli@takisbiotech.it (G. Roscilli), m.trombetta@unicampus.it (M. Trombetta), pamela.mozetic@cnr.it (P. Mozetic), a.rainer@unicampus.it (A. Rainer).
[1] Equally contributed.

https://doi.org/10.1016/j.biomaterials.2024.122482
Received 29 August 2023; Received in revised form 17 January 2024; Accepted 20 January 2024
Available online 22 January 2024

lymphocytes), and other tissue-resident cell types. Moreover, TME includes a non-cellular portion represented by the ECM components (e.g., collagen, fibronectin, laminin, and hyaluronan) and a complex network of soluble products, such as chemokines, cytokines, growth factors, enzymes, and extracellular vesicles, all of which contribute to tumor formation and maintenance. The cellular and non-cellular components of the TME play a crucial role in the generation of the complex network of signals involved in tumor progression [3,4].

Recent studies [5] suggest that anticancer treatment efficacy may also be influenced by the composition of the TME: therefore, understanding the cellular and molecular mechanisms inside the TME is essential to discover biological targets for the development of new anticancer strategies.

Microphysiological systems are *in vitro* miniaturized cell culture devices [6] which have emerged as a suitable tool to reproduce the complexity of the cellular microenvironment [1,7–11] with increased spatial and temporal control over the local cellular surroundings and to enable the controlled assembly and culture of cell clusters, down to single cells.

A clear example of these systems is represented by organs-on–chip (OoC), advanced *in vitro* tools capable of replicating the functional unit of an organ [12–14]. OoCs are an emerging technology for mimicking cell-cell and cell-ECM interactions with a higher degree of similarity to the pathophysiological conditions compared to classical *in vitro* models [15–18], while enabling experiment parallelization and compatibility to both standard biochemical techniques [13,19] and advanced microscopy tools [20]. Most of these devices are fabricated in polydimethylsiloxane (PDMS) using the replica molding technique. PDMS owes its large application to its biocompatibility, good gas permeability, and optical transparency. Moreover, its elastic behavior has been exploited to apply mechanical cues associated to organ pathophysiology [21,22]. However, PDMS is an intrinsically hydrophobic polymer showing a high level of protein adsorption. For this reason, recent research trends have reported the use of alternative polymers, such as nonabsorbent elastomers and transparent polyesters, to produce increasingly sophisticated and reliable platforms [23]. It is also worth noting that the recent advances in additive manufacturing (3D printing) processes have made them an attractive alternative to soft lithography for the fabrication of microfluidic cell culture devices [24,25], widening the range of applicable materials.

The organ-on-a-chip technology has been used to simulate a multitude of organs, including the heart, lung, liver, kidney, and the blood-brain barrier [26–30]. A recent comprehensive bibliometric analysis over the 10-year span [31], underscored the ever-increasing relevance of this research field. Notably, the keyword "tumor microenvironment" ranks first as the biological domain associated to OoC research. OoCs have indeed emerged as an enabling technology in cancer research (Tumor-on-Chip), with applications ranging from disease modeling to drug screening [32–34]. Cancer research is therefore witnessing a profound shift toward three-dimensional (3D) cell culture models, since the 3D arrangement has higher pathophysiological relevance compared to two-dimensional (2D) cultures [35]. 3D models have the advantage of

**Table 1**
Representative examples of TMOCs, classified into 2D/3D cell-laden and spheroid-based platforms.

| Platform | | Cell Lines | Matrices | Case studies | Drug Information |
|---|---|---|---|---|---|
| **2D/3D cell-laden platforms** | **Non vascularized platforms** | • Immune Cells [56–58]<br>• TCR-T cells [59]<br>• Cancer-associated fibroblasts (CAFs) [49–51]<br>• CAR-T [69]<br>• Human monocytes [59]<br>• A375 metastatic melanoma cells [58]<br>• HBV-HCC [59]<br>• Human mammary epithelial cells [41]<br>• Breast [41,49–51], Ovarian [69] cancer cells | • Collagen [49–51,56,59]<br>• Matrigel [58]<br>• Gelatin methacrylate [69] | • Cell migratory capability [41, 56–58]<br>• Drug studies [41,50,58]<br>• Tumor-stroma interactions [49,51]<br>• Antitumor activity of TCR-T cells [59]<br>• Cytotoxicity and infiltration of CAR-T cells in a hypoxic tumor [69] | • Paclitaxel [41]<br>• Tamoxifen [41]<br>• Suberoylanilide hydroxamic acid [50]<br>• Decitabine [58] |
| | **Vascularized platforms** | • Fibroblast [81,82,89,91]<br>• Endothelial cells [81–85, 89,91]<br>• Colorectal [81,85], Breast [81–83,89], Melanoma [81], Liver [85], Lung [85] cancer cells<br>• Patient-derived glioma stem cells [84]<br>• Monocytes [91] | • Fibrin [81,84,85,91]<br>• Glycol chitosan and benzaldehyde-modified polyethylene glycol [82]<br>• Collagen [82,83,89] | • Drug studies [81–85]<br>• Antibody-dependent cell-mediated cytotoxicity (ADCC) [89]<br>• Role of monocytes on cancer cell extravasation [91] | • Pazopanib [81]<br>• Paclitaxel [81]<br>• Doxorubicin [82,83]<br>• Plerixafor [84]<br>• Sunitinib [85] |
| **Spheroid-based platforms** | **Spheroid-based 3D tumor model** | • CAFs [115]<br>• Pancreatic stellate cells [116,117]<br>• M2 THP-1 [117]<br>• Immune cells [121]<br>• NK92-CD16 cells [121]<br>• Colorectal [115,118], Pancreatic [116,117,121], Breast [120,121] cancer cells | • Collagen [115–117,120]<br>• Matrigel [118,120,121] | • Drug screening [115–118, 120]<br>• Epithelial-to-mesenchymal transition [116,117]<br>• Hypoxic tumor model [120]<br>• ADCC [121] | • Paclitaxel [115–117]<br>• Gemcitabine [116,117]<br>• 5-fluorouracyl [117]<br>• Oxaliplatin [117]<br>• Irinotecan [118]<br>• AZD0156 [118]<br>• Doxorubicin [120] |
| | **Spheroid-based vascularized model microenvironment** | • Fibroblast [75,129,133, 137,138]<br>• Endothelial cells [75,129, 133,134,137,138]<br>• Ovarian [134], Lung [129, 134,137] cancer cells<br>• Esophageal carcinoma cells [138]<br>• ASPS cells [133] | • Collagen [75,129,133]<br>• Fibrin [75,129,133,134, 138]<br>• Hydrogel based on decellularized lung ECM mixed with collagen [137] | • Tumor behavior under intraluminal flow [75]<br>• Drug studies [75,129,134, 137,138]<br>• Neovascularization mechanism [133] | • Paclitaxel [75,134,138]<br>• Doxorubicin [129,137]<br>• Dimethyloxalylglycine [138]<br>• Cisplatin [138] |

precisely mimicking the organization of tissues in which cells grow [36]. By integrating 3D cultures within microfluidic devices, either as cell-laden hydrogels or cell spheroids/organoids, scientists have achieved an accurate monitoring of key signaling pathways involved in cell-cell and cell-ECM communications occurring in the TME [37] in a fashion closer to the *in vivo* settings.

This review illustrates one decade of progress in the field of tumor-microenvironment-on-chip (TMOC) models to gain insights into the pathophysiology of human cancer (Table 1). We will start from analyzing 2D/3D *in vitro* tumor models, and we will proceed to more sophisticated approaches highlighting the advantages of integrating the vascular component into 3D tumor models (Section 2). We will highlight how the increased degree of biomimicry offered by the most advanced TMOCs based on tumor spheroids (Section 3) has enabled scientists to investigate the role of microenvironmental factors and cellular interactions in tumor progression, invasion, and response to drug therapies. We will then overview the recent trend of integrating TMOCs into multi-organ systems (Section 4), with the final aim to follow the metastatic cascade to target organs and to investigate the effect of chemotherapeutic drugs from a systemic perspective. Lastly (Section 5), we will forecast forthcoming research trends in the field with a focus on technological and regulatory frameworks.

## 2. 2D/3D models

Several *in vitro* models have been developed to reproduce the complexity of the tumor microenvironment, exploiting microfabrication as an enabling technology. TMOC platforms mimic fundamental structural and functional characteristics of the TME by reproducing key specific aspects, such as biochemical gradients and dynamic cell-cell/cell-matrix interactions. Indeed, the TME is characterized by human-specific biophysical and biochemical factors that are difficult to reproduce in traditional *in vitro* and animal models. TMOCs enable simulating tumor growth and expansion [1], angiogenesis [37], and progression from early to advanced lesions involving epithelial-to-mesenchymal transition, tumor cell invasion, and metastasis [38].

In this section, we will analyze salient TMOC applications in which cells are inserted into microfluidic chambers either in 2D or encapsulated in ECM-mimicking hydrogels to achieve a 3D culture condition to better understand the underlying dynamic cellular interactions, exploiting ECM-mimicking matrixes, haptotactic gradients, and shear stress stimuli as adequate promoters for cell migration, intracellular signaling, proliferation and differentiation. Exploiting a combination of fluid flow and mechanical forces, TMOCs can influence cell shape, function, interaction and differentiation processes closely to the *in vivo* condition [39,40].

These models have the primary function of testing the effect of anticancer drugs in cell-cell interactions with a focus on cell motility, migration, and formation of vascular networks (Table 1).

### 2.1. Cell migration and invasion studies

Cell migration is a key process involved in different biological phenomena, including immune response and cancer progression, while invasion ability is a pivotal step in the metastatization pathway in which tumor cells spread through the circulatory and lymphatic systems and disseminate from the primary tumor to colonize distant organs. Both mechanisms are influenced by several physical, chemical, and molecular factors that need to be elucidated. To better understand these cellular features, it is necessary to overcome endpoint-based assays and move toward more efficient *in vitro* high-throughput studies taking advantage of live cell microscopy. Since the interaction of cancer and non-malignant cells influences cancer cell migration and response to drugs, TMOC models have been proposed to better understand these mechanisms. As an example, cancer cells migration was assessed using a microfluidic system for the co-culture of normal human mammary epithelial cells (HMEpiC) and MDA-MB-231 breast cancer cells [41]. This device was used to quantify cancer cells migration ability in mild, moderate and severe cancer models. To evaluate the role of non-malignant cells in tumor cell migration, cells were separately seeded in two culture chambers, endowed with pulsed pressure stimulation and interconnected via a microchannel array. When co-cultured with HMEpiC, cancer cells developed an increased migration ability, attributed to the increased secretion of IL-6. At the same time, cancer cells altered the phenotype of normal epithelial cells, which experienced morphological changes and decreased cytokeratin-14 secretion. The model could be used for the screening of anti-metastatic drugs, reporting a dose-dependent inhibition of tumor cells migration exerted by paclitaxel and tamoxifen.

The interaction between tumor and stroma significantly affects the formation of metastases, the progression of the disease [42,43] and the efficacy of target therapies [44]. Additionally, stromal cells, such as CAFs or bone marrow stromal cells, have been shown to endow the tumor with a resistance to therapeutic T lymphocytes [45,46]. The lack of stroma is a highly limiting factor in 2D tumor models considering that, in certain types of cancer, stroma is critical for tissue remodeling [47].

In this regard, a TMOC platform was used to evaluate the molecular and cellular basis of tumor-stroma interactions on cancer invasion [48]. Breast cancer cells (SUM-159, MDA-MB-231, MCF7) were embedded in collagen and co-cultured with patient-derived CAFs or normal fibroblasts [49]. CAFs increased the rate of breast cancer invasion into the 3D microenvironment by inducing expression of non-metastatic B-glycoprotein. Conversely, a reduced migratory and proliferative behavior of tumor cells was reported in association to normal fibroblasts. The same platform (Fig. 1A) had already been used in a previous work [50], where the role of suberoylanilide hydroxamic acid (SAHA), a histone deacetylase inhibitor, was investigated by examining phenotypic changes to of breast cancer cells co-cultured with CAFs. Following treatment with SAHA, cancer cells showed a more elongated shape and a significantly reduced migration velocity in the collagen matrix compared to untreated cells. Furthermore, the addition of CAFs to the tumor model enhanced tumor cell invasion without affecting drug resistance.

An intriguing alternative for the on-chip recapitulation of the tumor/stroma interaction is represented by the use of 3D microtissue precursors (3D-μTP) technology for the assembly of TMOCs [51]. 3D-μTPs are 3D cell constructs supported on porous gelatin microparticles (75–150 μm in diameter), achieved through spinner flask bioreactor conditioning and acting as the building blocks for microtissue assembly. An optically accessible microfluidic device was designed to host and interface the stromal and tumor compartments, which were filled with normal fibroblasts and breast cancer cells (MCF-7 line) 3D-μTPs, respectively, with the aim of replicating the modifications occurring in the healthy stroma during the invasion of malignant epithelial breast cells. Thanks to the ability of stromal cells in assembling their own ECM components, the model successfully replicated the pathophysiological dynamics occurring *in vivo* at the extracellular level and allowed the switch from a healthy to a pathologic ECM status to be monitored and quantified in real time.

### 2.2. Tumor-immune system interactions

One of the salient cellular components of the TME is represented by tumor-associated immune cells, which may exert tumor-antagonizing (e.g. $CD8^+$ and $CD4^+$ T cells, natural killer) or tumor-promoting functions (e.g. regulatory T cells and myeloid-derived suppressor cells). In the early stage of tumorigenesis, the tumor-antagonizing immune cells recognize and kill cancer cells. However, cancer cells have evolved a variety of mechanisms to escape from immune surveillance and cytotoxic function of the immune system [52]. In recent years, several immunotherapy strategies have been developed exploiting the tumor-associated immune cells in TME with high specificity in

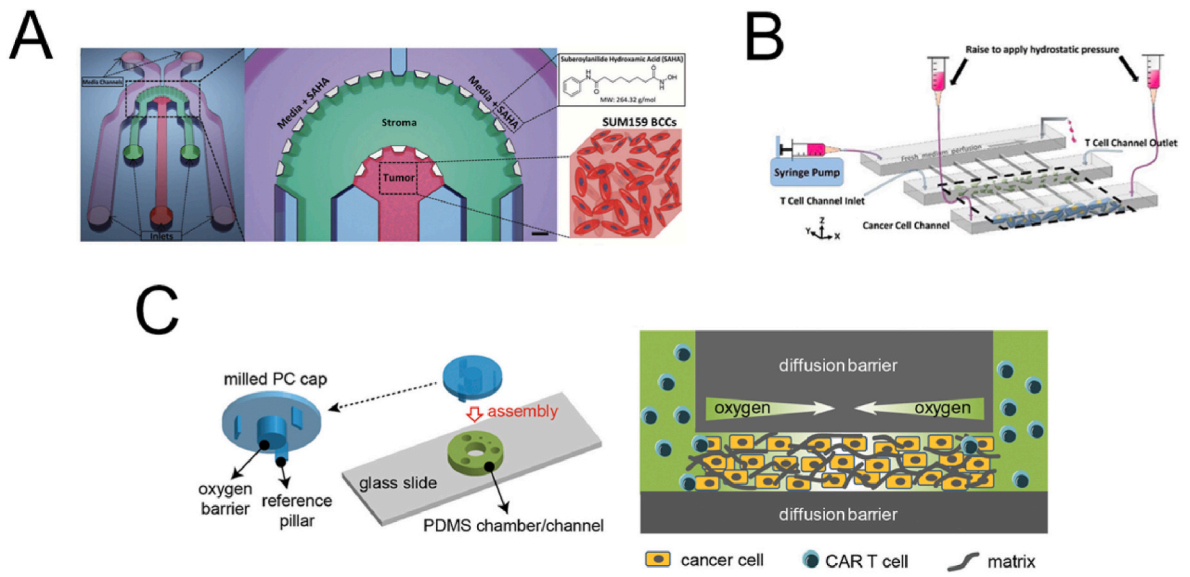


**Fig. 1.** *2D/3D TMOC platforms with a focus on cell-cell interaction. (A) Schematic representation of the platform developed to evaluate the effects of suberoylanilide hydroxamic acid on breast cancer. Adapted with permission from* Ref. [50]. *(B) Schematic representation of the platform to study the migration and antitumor response of tumor antigen-specific CTLs targeting liver cancer cells through antigen-specific and allogeneic recognition. Reproduced with permission from* Ref. [56]. *(C) Illustration of the working principle and assembly of the platform for the evaluation of cytotoxicity and infiltration of CAR-T cells in a hypoxic ovarian tumor. Adapted with permission from* Ref. [69].

recognizing cancer cells and lower side effects compared to traditional chemotherapeutic approaches.

As T lymphocytes play a pivotal role in immunity against tumor cells, their infiltration into the tumor microenvironment and the activation of effector T lymphocytes have been described as prognostic biomarkers for T-cell-based immunotherapies in different types of tumors [53–55]. However, several solid tumors are covered by a dense collagen capsule and possess increased interstitial fluid pressure (IFP), which represent physical barriers to anticancer immunotherapy.

The effect of the physical barriers characterizing the tumor interstitium was reproduced using a microfluidic platform in order to study the antitumor response of tumor antigen-specific cytotoxic T lymphocytes (CTLs) [56]. The physical constraints of the tumor interstitium were recreated by narrow entrances confined by a dense collagen capsule and high interstitial fluid pressure (achieved by imposing a hydrostatic pressure), which physically prevented CTL infiltration (Fig. 1B). The antigen specificity between CTLs and target tumor cells influenced the recruitment of CTLs into the surrounding tumor, but did not affect how CTLs infiltrated through the narrow tumor interstitium. However, the presence of physical barriers influenced the performance of the CTL-mediated antitumor response, as CTLs reached the tumor culture chamber in a longer time.

A TMOC model was also used to deepen the interpretation of *in vivo* data regarding chemotherapy-induced antitumor immune responses [57], with a focus on the role of formyl peptide receptor 1 (FPR1). The chip featured two chambers, hosting tumor cells and immune cells, respectively, separated by an array of narrow capillary migration micro-channels. Mouse splenocytes (WT or FPR1$^{-/-}$) or human PBMCs (from WT, heterozygous or mutated homozygous subjects) were separately tested against cancer cells, pretreated or not with anthracyclines. By tracking immune cell infiltration and by quantifying the interaction times with cancer cells, it could be observed that FPR1 was associated with stable interactions of immune cells with anthracycline-treated dying cancer cells. A similar approach was applied to address the immune escape phenomena in melanoma [58]. Human PBMCs were loaded in a microfluidic channel, flanked by two Matrigel-laden parallel chambers for the 3D culture of A375 metastatic melanoma cells, pre-treated or not with the DNA demethylating agent decitabine and with interferon-α, alone or in combination. By tracking and quantifying the infiltration of PBMCs toward the tumor chamber, the authors reported that the drug combination was effective in circumventing the immune escape mechanisms of melanoma cells.

One of the most advanced therapeutic options in the field of immunotherapy is represented by adoptive cell therapy, which endows T cells with the ability to recognize and kill cancer cells through cell engineering. In this regard, a microfluidic platform was designed to assess the antitumor activity of T cell receptor (TCR) engineered T cells (TCR-T) against a 3D model of HBV-HCC (hepatocellular carcinoma expressing hepatitis B antigen) in the presence of immunosuppressive monocytes [59,60]. The microfluidic device consisted of a central channel with human monocytes and HBV-HCC 3D aggregates embedded in collagen gel mimicking the intrahepatic carcinoma environment, and two adjacent channels in which TCR-T cells were perfused. The model outperformed static 2D control models, also discriminating the performance of TCR-T cells produced by different methods (retroviral transduction vs. mRNA electroporation).

Solid tumors are also often characterized by a hypoxic TME, due to the presence of abnormal vascular structures and to the influence of tumor cells metabolism. Hypoxia is a TME factor known to play a key role in cancer progression and immune editing, with cancer cells adapting to the hypoxic environment and eliciting a series of responses [61]. Activation of hypoxia-inducible factor 1 alpha (HIF-1α) is associated with inhibition of anti-tumor cytokines TNF and IFN-γ [62], PD-L1 upregulation [63], and enhanced secretion of immunosuppressive cytokines [64–68].

A hypoxic 3D tumor model was reproduced in a microfluidic platform for the study of chimeric antigen receptor T cells (CAR-T) antitumor mechanisms [69], considering that the hypoxic environment is known to hinder T cell infiltration and functionality in solid tumors. Following a previously validated chip design [70], the device was endowed with a barrier to oxygen diffusion and with fluorescent silica-microbead-based oxygen sensors for real-time monitoring of hypoxic conditions. Ovarian cancer cells in gelatin methacrylate (GelMA) matrix were confined in the chip, while CAR-T cells were inserted into a channel adjacent to the tumor chamber (Fig. 1C). Results showed the achievement of a significant oxygen gradient in the tumor, with enhanced cell killing by CAR-T cells, despite the evidence of increased immunosuppression under these conditions.

To gain a more comprehensive insight on the dynamics of human TME, it is necessary to introduce additional components, such as intraluminal flow into a vascular network, to mimic the effects of blood flow on tumors [71]. Hence, vascularized microfluidic platforms have been developed to evaluate the proliferation of tumor cells and the effectiveness of therapeutic strategies under perfusion conditions, since extracellular transport and fluid shear stress can influence the development of drug resistance mechanisms [72].

### 2.3. Integration of the vascular component

The blood vessels within the tumor exhibit disarray, twisting irregularly and allowing leakage, leading to elevated pressure and reduced oxygen levels in the tumor microenvironment. These conditions contribute to the facilitation of tumor growth and the sustenance of the tumor survival [73,74]. Furthermore, the rapid growth of the tumor causes a mechanical compression on the cancer-associated vascular network that enhances the interstitial fluid pressure (IFP) in the tumor tissue. This enhanced fluid pressure increases the invasive characteristics of tumor cells promoting the metastatization process and hinders the effective delivery of drugs to the tumors [75,76]. Based on these mechanisms, tumor-associated blood vessels have gained importance as a therapeutic target in the treatment of metastatic tumors [77].

Engineered microvessels can be exploited as a tool for the study of tumor growth and metastatic mechanisms in drug screening studies and anticancer therapies design [38]. Literature reports the development of vascular structure models, including functional vascular networks grown in 3D matrices (collagen, fibrin, hyaluronic acid [78]) and endothelial cells seeded in microfluidic channels with flow-induced shear stress to reproduce the capillary endothelium [71].

Leveraging microfluidics, 3D engineered microvascular network models can be representative of tumor-associated microvasculature in a precise and reproducible manner [72], also serving as a tool for the assessment of anticancer therapies, given that drugs and immune cells traverse through the vascular system [73].

#### 2.3.1. Drug transport and effect studies on vascularized TMOCs

Drug transport within solid tumors is influenced by several factors, including the tumor-associated vasculature. Tumor vasculature is characterized by high heterogeneity in its structure and density within the solid mass; generally, the tumor core is avascular and necrotic, while the presence of blood vessels increases towards the periphery. Moreover, these defective architecture of blood vessels, known as a "leaky vasculature", could hinder anticancer drug diffusion [79,80].

vivoTo test the sensitivity of vascularized tumors to chemotherapeutic drugs, different vascularized solid tumors have been modeled using a microfluidic platform incorporating both tumor (breast, colorectal, and melanoma cancer cell lines) and stromal cells (human lung fibroblasts) growing in an ECM-mimicking 3D matrix and depending for survival on a perfused microvascular network (cord-blood-derived endothelial cells) [81]. The chip layout featured two straight medium supply channels separated by an array of three diamond-shaped chambers for cell culture, connected to the channels through capillary burst valves (Fig. 2A). Upon culture, endothelial cells self-organized into a microvasculature structure, reaching anastomosis with the medium supply channels, thereby supporting physiologic flow and delivering nutrients to surrounding cells. Results also showed sensitivity of the microvessels to anti-angiogenic (pazopanib, linifanib, cabozantinib, axitinib, etc.) and vascular disrupting agents (vincristine, paclitaxel), suggesting the potential use of the platform for the screening of treatments targeting cancer through effects on the vasculature.

An alternative design to evaluate the effects of anticancer drugs on a vascularized TME has been proposed [82], with the aim to investigate the effects of doxorubicin on sensitive and resistant breast tumor cells. The microfluidic platform featured a porous polycarbonate membrane separating an upper layer (formed by two cell culture compartments separated by a PDMS wall) from a lower layer, consisting of a wide perfusion channel (Fig. 2B). To mimic the vascularized TME, NIH-3T3 fibroblasts and HUVEC were separately seeded on the upper and lower sides of the membrane. Tumor cells, namely MCF7 line and its adriamycin-resistant variant (MCF7/ADR), were separately suspended in a hydrogel matrix (composed of glycol chitosan and benzaldehyde-modified polyethylene glycol) and seeded in the cell culture compartments. The lower channel mimicking a blood vessel was used for the administration of doxorubicin. The hydrogel played a supporting role for long-term cell culture and for cell-to-cell and cell-ECM crosstalk. In co-culture conditions, MCF7/ADR resistant cells showed an enhanced resistance to doxorubicin treatment compared to mono-culture conditions.

TMOCs also offer an amenable platform for the screening of

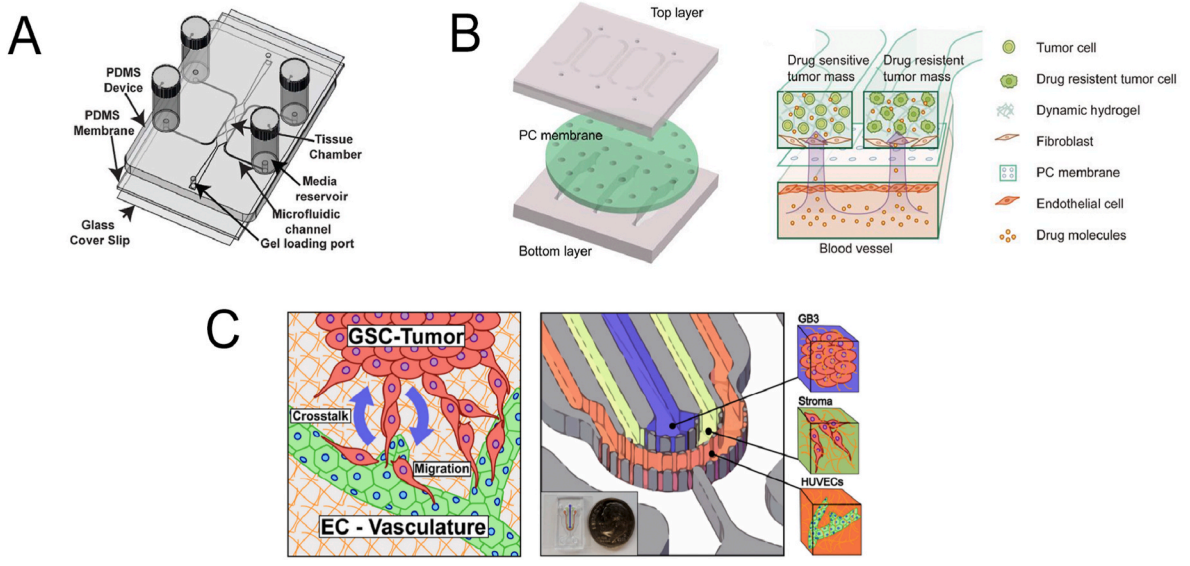


**Fig. 2.** *Microfluidic platforms featuring engineered microvessels to study tumor growth and metastasis mechanisms. (A) Schematic representation of the platform for achieving vascularized micro-tumors. Adapted with permission from* Ref. [81]. *(B) Schematic representation of bilayer platform to investigate the effects of doxorubicin on sensitive and resistant breast cancer cells. Adapted with permission from* Ref. [82]. *(C) Schematic representation of the platform to recapitulate the glioblastoma tumor niche. Adapted with permission from* Ref. [84].

nanomedicine approaches, as in the case of nanoparticle-vehicled doxorubicin in breast cancer [83]. The chip featured a lower layer with a main chamber in which tumor cells (either MCF7 or MDA-MB-231) were grown in a collagen matrix. In addition, two lateral channels, separated from the interstitial channel through equidistant pins, simulated the passive drainage to the lymphatic system. The upper layer featured a microfluidic channel reproducing a capillary of the tumor micro-vascularization, separated from the main chamber by a porous membrane mimicking the capillary wall. Culture medium (supplemented with doxorubicin) was supplied through the capillary channel into the hydrogel, mimicking the interstitial fluid pressure encountered in an *in vivo* setting. To demonstrate the advantages of the TMOC platform for drug screening, the phenotypic changes of cells grown in the microfluidic model were compared to those of a classical 2D cell culture upon doxorubicin administration. In all the experimental conditions, cells cultured in the TMOC platform showed higher drug resistance compared to the 2D controls.

Multi-layered microfluidic platforms have been employed to investigate the contribution of the vascular compartment to tumor growth [84]. Specifically, a three-layer microfluidic platform was developed to study how the perivascular component influences the stemness of glioma cells and to evaluate the effect of the drug AMD-3100 (plerixafor) on their invasive behavior [84]. The 3D microvascular network was built by injecting a suspension of HUVECs in fibrin into the vascular region of the platform, while patient-derived glioma stem cells were seeded into the tumor region (Fig. 2C). The cellular crosstalk within the perivascular region induced glioma stem cells to acquire an invasive phenotype, which was reduced following treatment with AMD-3100.

Vascularized platforms also represent a useful tool to recapitulate 3D angiogenic sprouting in the TME. As an example, a multi-chamber device featuring five parallel channels separated by micro-post arrays was used to validate mesoporous silica nanoparticles as a delivery system for siRNAs targeting the VEGF receptor (siVEGFR) [85]. Two central channels were filled with tumor cells (HepG2, SW620, and A549) embedded in fibrin gel and acellular fibrin gel, respectively, the latter to be used for angiogenic sprout formation. HUVECs were cultured in a channel adjacent to the acellular hydrogel channel. On the other side, a medium channel separated the tumor chamber from the 3D culture of stromal fibroblasts, which provided the system with a basal level of pro-angiogenic factors [86]. The above-described models highlight the central role of the vascular network in regulating the mechanisms of cancer cell migration and invasion and cancer response to drugs [87]. Although these results have led to significant advancements in the field, there are still some aspects to be elucidated. These include, for example, understanding the spatiotemporal distribution of angiogenetic signals and their effect on the formation of a stable microvasculature suitable for pharma R&D investigations [88], as well as describing the effects of perfusion-induced shear stress on endothelial cells.

#### 2.3.2. Immunocompetent vascularized TMOC models

A further improvement in the recapitulation of the TME is represented by the generation of immunocompetent vascularized TMOC platforms.

An *ex vivo* immunocompetent TME model was recreated in a microfluidic platform specifically designed to integrate four different cell populations (cancer cells, immune cells, vascular endothelial cells, and fibroblasts) [89]. The central chamber hosted an endothelial cell monolayer, while the two lateral chambers were filled with collagen I hydrogel laden with tumor cells (the HER2-positive breast cancer BT474 cell line) and fibroblasts, together with immune cells. The model was validated by studying the effect of Herceptin (trastuzumab), an antibody directed against the HER2 receptor, on the TME. By binding to upregulated HER2 receptors on tumor cells, trastuzumab created multiple binding sites for receptors expressed on the surface of different subtypes of immune cells, including natural killer cells, B lymphocytes, dendritic cells, and macrophages, recapitulating an antibody-dependent cell-mediated cytotoxicity (ADCC) immune response. The system also revealed the pro-invasive and immunomodulatory roles of CAFs, which may also contribute to cancer resistance toward trastuzumab. Overall, the immunocompetent TME model was successful in recapitulating *in vitro* the complex interaction observed using *in vivo* models.

Macrophages have been extensively described to support cancer progression providing support for extravasation and survival of metastatic cell [90]. More recently, attention was drawn at the role of monocytes, as precursors to macrophages, in cancer progression. In this regard, a microfluidic model was proposed to study the role of monocytes on cancer cell extravasation [91]. The chip featured a main chamber in which a suspension of human fibroblasts and endothelial cells in fibrin gel was cultured in 3D fashion leading to the self-assembly of a 3D microvascular network. The chamber was flanked by two perfusion channels, through which monocytes and cancer cells were perfused in the microvasculature network, either simultaneously or in sequence. Results showed that, when perfused in association to cancer cells, monocytes reduced cancer cell extravasation in a non-contact dependent manner. Conversely, once monocytes transmigrated to the stromal compartment and acquired a macrophage-like phenotype, they had little effect on cancer cell extravasation.

## 3. Spheroid-based TMOC platforms

Among 3D cell models, spheroids, defined as self-assembled 3D cell aggregates [92] are largely used to study solid tumor biology since they reproduce several *in vivo* features of tumors. Spheroids are regarded as a more reliable model for various applications, including drug screening and cancer mechanism studies. Indeed, they exhibit similar proliferation rate, metabolic profile, and concentration gradients of *in vivo* tumors. Spheroids also exhibit cell-cell and cell-ECM interactions and accurately mimic the drug resistance mechanisms observed *in vivo* [36]. Moreover, spheroids present several advantages since they are clonal, simple to expand into large cultures and suitable for high-throughput systems. Spheroids can be obtained starting from cancer cell lines or cells isolated from patients; their formation occurs when cell suspensions are grown in the absence of an attachment surface, allowing cell-cell interactions to overcome cell-substrate ones. Several strategies have been developed for 3D cell culture, including the hanging drop method, round-bottom low attachment plates, and micro-patterned plates [93,94]. However, these culture methods show several shortcomings, mainly associated to scarce control over size and geometry of the spheroids and handling issues which result in well-to-well variability and difficulties for long-term culture.

In this section, we will start by highlighting how microfluidic platforms can be exploited to enhance cancer spheroids formation, handling, and analysis. We will then focus on the most salient spheroid-based TMOC approaches to recapitulate the TME (Table 1).

### 3.1. Microfluidics-assisted spheroid generation, manipulation, and culture

Microfluidics has emerged as an alternative to traditional techniques for spheroid formation and culture, especially regarding the possibility of miniaturizing the whole experimental procedure. This is an important feature in studies based on biopsies from cancer patients due to the lack of source material.

Different microfluidic devices have been used to obtain spheroids starting from established cell lines overcoming the limitations of classical methods for spheroid generation, resulting in simpler and more reproducible assays for anti-cancer drugs testing [95]. Microwell arrays represent a viable approach for generating cancer spheroids and testing their response to chemotherapeutic drugs [96], as reported for the generation of ovarian cancer spheroids. The device featured a multi-chamber design, with spheroid formation occurring due to sedimentation of cells in small, confined microwells of ca. 250 μm diameter and 300 μm in depth located in each chamber. Thanks to a set of

microfluidic valves, the device featured differential flow control modalities, allowing for serial flow control for seeding cells and parallel flow control for independent drug administration in each chamber. The device was validated by testing different concentrations of doxorubicin to determine the $IC_{50}$ values on an infusion of about 100,000 cells, considering this number as the lower number of cells present in fine-needle aspirate biopsy specimens.

Microfluidic devices were also successfully applied to the isolation of spheroids directly from primary tumor samples [97] using trapping unit arrays. The PDMS device comprised two inlets, a main chamber with spheroid isolation units and two outlets (Fig. 3A). A suspension containing spheroids from KPC mice primary pancreatic tumor explants was injected through the device to isolate relevant-size spheroids from single cells for further analysis and characterization. Spheroids were trapped in funnel-shaped isolation units with a large opening in the front and a small opening at the end, large enough to allow single cells to pass over. Spheroid isolation units could be modified in accordance with the dimension of the spheroids of interest. The isolated spheroids could be released from the device, tested for cell-specific markers, and cultured in 96-well plates for up to 14 days. Working from primary tumor explants enabled the isolation of spheroids containing a heterogeneous population of cells consisting of tumor cells, macrophages and fibroblasts, which preserved most of the *in vivo* features of the tissue.

Microfluidics has also been applied to ameliorate the efficiency of the classical hanging drop technique for spheroid formation. According to the technique, a defined number of cells is seeded into hanging drops of culture medium where cells sediment by gravity and aggregate to form a scaffold-free 3D spheroid. However, long-term culture and analysis requires several liquid handling procedures to be performed with accurate pipetting to avoid touching or destroying the spheroids. This issue has been addressed by the introduction of a finger-actuated hanging drop array (HDA) chip, which does not require external equipment or manual pipetting for cell seeding or subsequent culture steps [98]. The microfluidic device consisted of a multi-layer PDMS body assembled to form a 3x3 HDA, in which each row was fluidically independent and connected to finger-actuated pumping units operated by push buttons for medium supply or withdrawal. As a proof-of-concept, BT474 breast cancer cells were loaded into the HDA device to form spheroids which were cultured for 7 days, with daily medium exchange, and Live/Dead assay was performed directly inside the HDA device. Furthermore, spheroids were successfully embedded in a collagen matrix to mimic a metastatic environment by loading a collagen solution in the microfluidic channels.

To enable more complex multi-tissue studies, in which spheroids derived from different cell types could be fluidically interconnected, a hanging drop network (HDN) platform was developed for the formation, culture, and interaction of spheroids from different cell populations

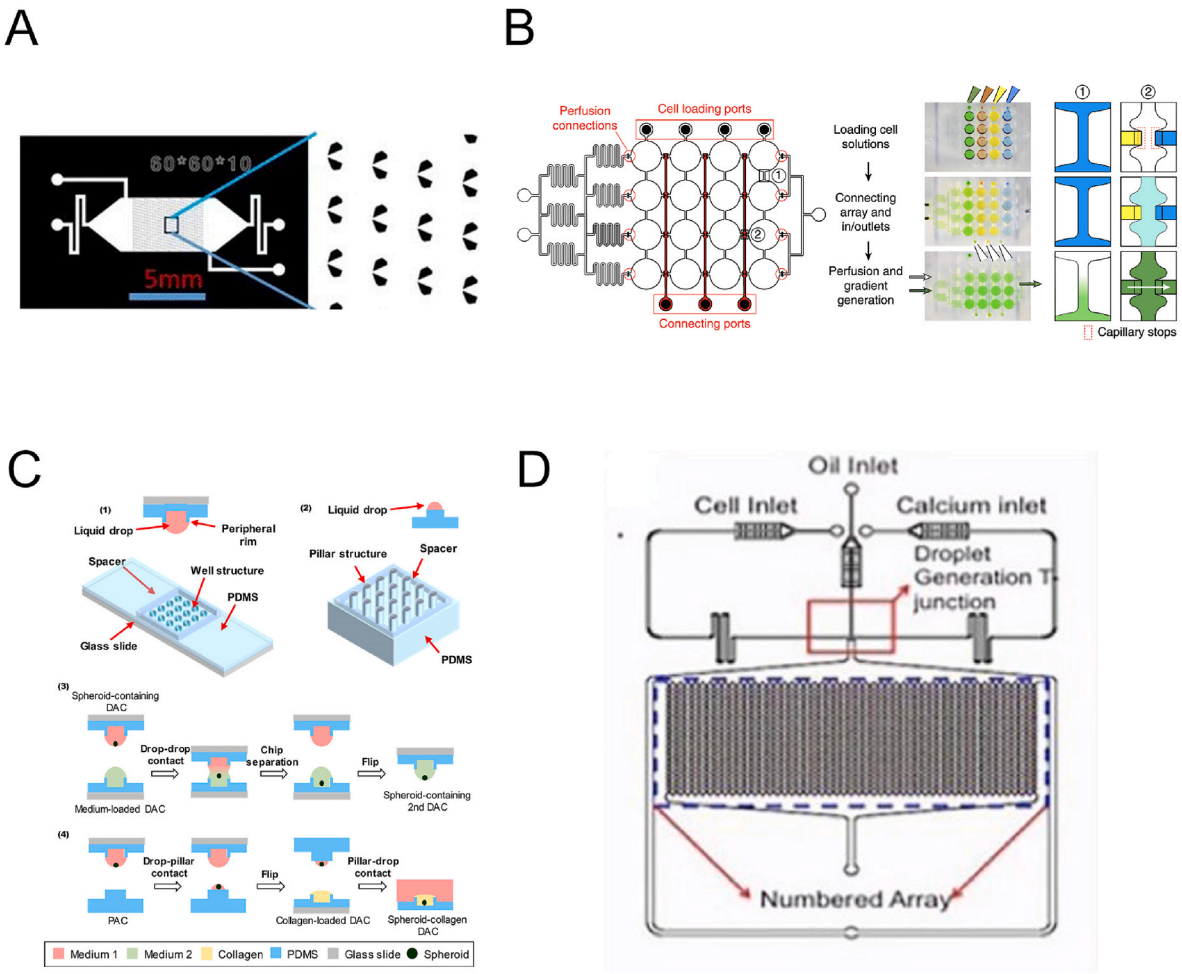


**Fig. 3.** *Platforms for microfluidic-assisted fabrication, manipulation, and culture of tumor spheroids. (A) Layout of the spheroid isolation device with a main chamber with hundreds of spheroid isolation units. Adapted with permission from* Ref. [97]. *(B) Schematic representation and working principle of the hanging drop network device for generation and co-culture of spheroids from different sources. Adapted with permission from* Ref. [99]. *(C) PDMS-based array for the droplet contact-based transfer methods: 3D sketch of the drop array chip (DAC) and pillar array chip (PAC) and illustration of the contacting method for medium change and the embedment of spheroid into collagen matrix. Adapted with permission from* Ref. [104]. *(D) Microfluidic device for cell encapsulation and spheroid localization in a docking array. Adapted with permission from* Ref. [109].

under controlled flow conditions to recapitulate the behavior of organ networks [99] (Fig. 3B). The platform featured an open microfluidic network located at the bottom of a substrate, in which the hanging-drop structures were faced downwards. The channel layout was defined by hydrophobic rims, so that liquid distribution could be controlled by capillary and surface tension forces. The HDN was constituted by an array of circular patterns for the formation of hanging drops interconnected through short connection channels. Capillary valves were used to achieve on-demand reconfiguration of the connections between adjacent hanging drops, and dedicated cell loading ports enabled the generation of spheroids from different cell types which could be then fluidically connected under perfusion with gradient generation.

An alternative microfluidic implementation of the hanging drop principle is represented by the SimpleDrop chip, a micro-hole device for the culture and analysis of 3D spheroids [100]. The device was composed of a PDMS layer, punched with a flat needle to form holes with large extremities and a narrow middle section, in which the cell suspension was introduced and formed drops. Cells aggregated inside the droplets due to gravity forces and formed a 3D spheroid within 24 h. Spheroids could be maintained in the device for long term culture (up to nine days). The system could also be used for the administration of drugs or functional probes to tumor spheroids, enabling its application in drug screening and viability studies. As an example, different concentrations of cisplatin, paclitaxel and methotrexate were tested on HS-SY-II spheroids cultured in the SimpleDrop device and their anticancer effects were evaluated by fluorescence microscopy.

When spheroids are obtained by culturing cells in suspension, for example using the hanging drop method or round-bottom 96-well plates, they lack interaction with the ECM, which is crucial for different cellular functions [95]. Therefore, after their formation, spheroids can be embedded in hydrogels to mimic *in vivo* cell-ECM interactions or metastasis formation. Exogenous ECM can be obtained using different biomaterials (e.g., collagen, alginate, gelatin, Matrigel), and its composition can be modified to tune matrix stiffness and permeability, with consequent effects on nutrient transport and mechanical properties of the tumor microenvironment. Spheroids-in-hydrogel models are widely used in cancer studies, but the embedment of spheroids in the hydrogel is an intricate process, since it requires manual handling of single spheroids, hence hindering the application in high-throughput screening studies.

An advancement in the field is represented by the introduction of a microfluidic device to downsize drug sensitivity assays on collagen-embedded spheroids [101]. The chip featured three sections, each composed of two media channels surrounding a central gel channel, in which spheroids were seeded after being resuspended in collagen mixture. The device was used to perform a drug sensitivity assay on HK-1 nasopharyngeal cancer cell spheroids. Results were in agreement with those obtained on control groups of collagen-embedded spheroids cultured in 24-well plates, while the setup time and the amount of collagen were significantly reduced, paving the way to cheaper high-throughput studies.

Classical microfluidic techniques for hydrogel patterning, such as surface-tension-based patterning [102], exploit intermittent physical barriers, such as micropillars or narrow openings, which cause a discontinuous cell-ECM interface. A "pillar-free" device was developed using a stepped-height-based hydrogel patterning method [103]. The method represents an on-chip spheroid-in-gel formation process, achieved by combining a hanging drop-based spheroid formation phase and a hydrogel patterning phase. The chip consisted of a PDMS substrate endowed with parallel microfluidic channels, each featuring individual extruded islands (lower in height than the channels) for cell/hydrogel confinement. To obtain spheroids, a cancer cell suspension was directly loaded onto the islands, confined as a droplet and cultured "upside--down" for spheroid formation. Upon spheroid formation, medium could be replaced by a hydrogel to encapsulate the spheroids. The chip could then be faced to a glass substrate achieving hydrogel confinement in a single "press-on" step. Although the method eased the access to spheroid-based models, it presented some limitations regarding spheroid numerosity, dimensions and culture time span.

To overcome these limitations, an advanced cell culture device implementing a "droplet contact-based spheroid transfer" (DCST) technique was proposed. The platform was conceived to embed spheroids in collagen drops and to facilitate medium exchange process in long-term experiments [104–106] by sequential contacting procedures between patterned substrates hosting the spheroids and confined aliquots of medium/hydrogel (Fig. 3C). The original DCST device was further improved by introducing 3D-printed molds to obtain more stable spheroids during multiple reagent addition or washing steps in multi-step spheroid assays [105]. The improved DCST device was used as a platform to culture fibroblast-associated glioblastoma spheroids, demonstrating its suitability for high-throughput drug screening and personalized cancer treatments [106].

Droplet-based microfluidic systems represent another viable approach for the generation and embedment of spheroids. In particular, the implementation of flow-focusing strategies has been reported for the generation of high numbers of cancer spheroids of controlled size for high throughput imaging and analysis [107–110]. A salient example is represented by the two-section device developed to generate and host breast cancer spheroids [109]. The device was composed of a droplet generator and a docking microarray with holding sites for spheroids (Fig. 3D). Droplets were formed through a T-junction configuration, using a cell suspension in 2 % alginate as the internal phase and mineral oil as the external phase. Cell-laden droplets were trapped in the docking array where *in situ* gelation occurred by calcium ions, leading to stable alginate-embedded spheroids. Targeting the recapitulation of the TME, the platform was validated for long-term co-culture of MCF-7 spheroids with HS-5 bone marrow fibroblasts. In another work, the same microfluidic platform was applied to the generation of 3D tumor-stromal-immune cell spheroids [110] consisting of three cell types: a diffuse large B-cell lymphoma (DLBCL) cancer cell line, HS-5 fibroblasts and PBMCs formed in a hydrogel composed of alginate and PuraMatrix, a synthetic peptide resembling the ECM structure. Spheroids were treated with the immunomodulatory drug lenalidomide to evaluate cell response to immunotherapy; the treatment had an anti-proliferative effect on cancer cells and reduced the expression of several pro-inflammatory chemokines.

The use of hydrogels as a medium for direct cell embedding has the drawback of limiting cell-cell interaction, which is a prerequisite for spheroid formation. Scaffold-free methods, in contrast, are permissive for initial cell aggregation; however, the process may be influenced by differential levels of cell adhesion molecules (CAMs), leading to heterogeneities in spheroid formation, especially when multiple cell types are involved [111]. To overcome this limitation, droplet microfluidics and cell membrane engineering have been combined to promote the high-efficiency generation of multicellular tumor spheroids [112], using a chip endowed with an initial "cell aggregation" section, followed by a "spheroid formation" section. Cells were modified by installing biotin on cell membrane proteins using an N-hydroxysuccinimide (NHS)-activated biotin reagent. Modified cells were supplied to one side of a Y-shaped chip inlet, while the other branch was fed with streptavidin-containing medium. Streptavidin, with four biotin-binding sites, served as a bridge to enable robust cell-to-cell adhesion, resulting in the formation of (loose) cell aggregates. Aggregates then entered the following chip section, where encapsulation in alginate hydrogel microcapsules occurred according to a flow-focusing design. Microcapsules could be retrieved from the emulsion and cultured up to three days for spheroid formation. The approach was successfully validated for several cancer cell lines (HCT116, A549, and HepG2 cells), also including co-culture with fibroblasts (NIH-3T3). The artificial cell adhesion strategy was reported to prevent cell anoikis and synchronized the period of spheroid formation among different cell types.

The generation of multicellular spheroids was also addressed by Sun

et al., who chose to recapitulate the tumor/stroma interface in breast cancer [113]. By implementing a dual cross-junction flow-focusing process, the authors fabricated highly homogeneous core-shell particles featuring a scaffold-free core, laden with MCF-7 breast cancer cells, and an alginate shell containing human mammary fibroblasts. After *in vitro* conditioning, the particles resulted in tumor spheroids evenly coated by a stromal layer.

### 3.2. TMOCs integrating cancer spheroids

Tissue-like 3D models have the potential to increase the predictive value of *in vitro* models, reflecting the effects of TME features on cancer response to drugs [114]. One of the main advantages in the use of microfluidic devices integrating tumor spheroids is the possibility to reproduce the 3D interaction of the tumor with other microenvironmental components at the microscale level. As an example, an indirect co-culture microfluidic chip was designed to avoid the direct contact between tumor and stromal cells, allowing soluble factors to be transported across the medium channels so that local concentration gradients could be established [115]. In this model, HT29 human colorectal carcinoma cells were grown as tumor spheroids in collagen-laden channels and co-cultured with CAFs to mimic the *in vivo* mutual cell interaction. The microfluidic culture device was formed by four independent units, each featuring three cell-culture channels separated by medium channels, as shown in Fig. 4A. Cell morphology, proliferation, migration, and protein expression could be monitored during the co-culture period, revealing cell phenotypic changes for both cancer cells and stromal fibroblasts, mimicking mutual microenvironmental interactions. Additionally, HT29 spheroids were treated with paclitaxel to test its anti-proliferative activity, showing a survival advantage for spheroids co-cultured with fibroblasts compared to spheroids in monoculture.

In a following study [116], the same microfluidic device was used to develop a 3D pancreatic cancer model by co-culturing pancreatic tumor (PANC-1) spheroids with pancreatic stellate cells (PSCs), which represent the major source of CAFs in pancreatic ductal adenocarcinoma. Features of the TME were reproduced by culturing cells in a collagen matrix with the purpose of studying the epithelial-to-mesenchymal transition (EMT) and drug resistance mechanisms. Under co-culture conditions, both pancreatic spheroids and PSCs acquired an activated phenotype, with effects on cell growth and motility. The 3D reciprocal activation between the two cell types was confirmed by increased expression of EMT markers in tumor spheroids under co-culture. Also, a supra-additive effect on tumor cell viability was reported for the combination treatment with gemcitabine and paclitaxel. The synergistic effect of the treatment was attributed not only to the direct cytotoxic effect of paclitaxel on cancer cells, but also to the depletion of the peritumoral desmoplastic stroma and the consequent increased intratumoral gemcitabine levels.

The model was further refined by the addition of the immune component, represented by THP-1 derived M2 macrophages (M2 THP-1) [117]. Co-culture with stromal cells, such as activated PSCs and M2 THP-1, resulted in increased expression of expression of EMT-related proteins in pancreatic spheroids and promoted the invasion and migration of PANC-1 cells, while no increased drug resistance could be measured.

Although microfluidic/microfabricated devices represent an advanced experimental strategy for *in vitro* anticancer drug discovery and screening, many designs fail to reproduce the physiological exposure to drugs or to mimic the *in vivo* pharmacokinetic profile. To address this issue, an experimental setup was conceived to precisely impose a drug pharmacokinetic profile to tumor spheroids cultured on-chip [118]. The setup relied on a pump-driven system for the sequential delivery of specific drugs at a constant flow rate on Matrigel-encapsulated spheroids. The platform could mimic various therapeutic schedules—*e.g.*, monotherapy/combinatorial therapies or intermittent/continuous administration—and reproduce the drug

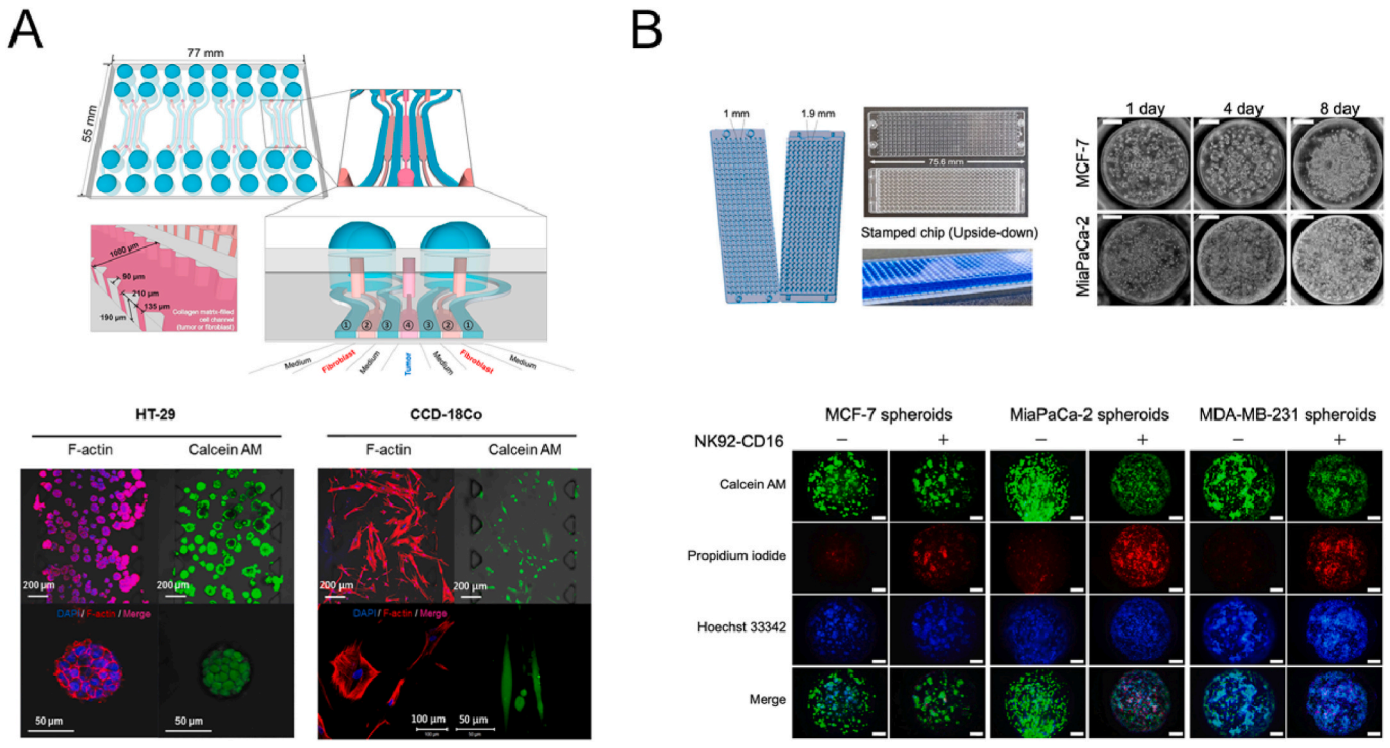


**Fig. 4.** *Spheroid-based TMOCs. (A) Microfluidic chip for the co-culture of colorectal cancer spheroids with fibroblasts. Schematic representation of chip layout (top) and fluorescence images of HT-29 spheroids and CCD-18Co fibroblasts (bottom). Adapted with permission from* Ref. [115]*; (B) Micropillar/microwell sandwich chip for ADCC studies on tumor spheroids. Chip layout and micrographs of tumor spheroids formed on the micropillar tips (top); image-based ADCC quantification (bottom). Adapted with permission from* Ref. [121].

plasma concentration decrease over time. As a proof-of-concept study, the platform was used to test the effect of irinotecan, a topoisomerase I inhibitor, and its combination with AZD0156 (an ATM kinase inhibitor) on SW620 colorectal cancer spheroids using concentrations similar to mouse plasma exposure profiles. The system could effectively replicate *in vivo* evidence, suggesting its applicability for drug pharmacodynamics studies.

The reported examples underline the importance of recapitulating the TME features to achieve more realistic tumor models in terms of cell response to drugs.

#### 3.2.1. Spheroid-based hypoxic models

As already evidenced in §2.2, hypoxia is a key factor of the TME, known to contribute to cancer radio- and chemo-resistance mechanisms [119]. To explore the tumor behavior under different oxygen conditions, a microfluidic culture device was designed to observe tumor spheroid responses to anti-cancer treatment [120]. The microfluidic device was composed of 3 layers: (i) a bottom layer consisting of a culture channel with an array of traps for spheroid-containing hydrogel beads surrounded by hydration and gas channels; (ii) an intermediate hydration layer for PBS perfusion to reduce media evaporation during oxygen control; and (iii) an upper gas control layer. Alginate-based beads, containing type I collagen and Matrigel and incorporating breast cancer MCF-7 spheroids, were trapped on-chip for spheroid exposure to different cycling oxygen profiles (0 %, 3 % and 10 %) at different time intervals. Spheroids showed a size variation driven by the swelling/-shrinkage of individual cells in response to different oxygen profiles. The system was also used to monitor the uptake and accumulation of doxorubicin under different oxygen conditions, from anoxic conditions (0 %) to *in vitro* normoxia (20 %). An increased doxorubicin uptake was reported for cyclic conditions, exceeding those of chronic hypoxia and normoxia. Additionally, a marked heterogeneity in drug uptake was observed within single cells composing the spheroids, with an intensity gradient from the spheroid edge to the center.

Solid tumor hypoxic conditions were also successfully recapitulated in a 3D co-culture of NK92-CD16 cells with pancreatic (MiaPaCa-2) and breast cancer (MCF-7 and MDA-MB-231) spheroids using a 330-micropillar/microwell sandwich chip. The device was used to study NK-cell mediated cell cytotoxicity in combination with two monoclonal antibodies (trastuzumab and atezolizumab) [121]. The platform was also used to observe cancer spheroids behavior after treatment with the chemotherapeutic drug paclitaxel in association, or not, with NK92-CD16 cells and the antibodies. To achieve tumor spheroid formation, tumor cells were resuspended in Matrigel and spotted on the tip of polydopamine-coated micropillars using an automated cell spotter. After polymerization, the micropillar chip was sandwiched with the corresponding microwell chip, where co-culture with NK cells took place. The chip enabled recapitulation of the dose-response behavior of cancer cells in hypoxic condition, which often induce resistance of target cells to therapeutics, demonstrating high sensitivity for paclitaxel when treated with both NK cells and antibody (Fig. 4B).

#### 3.2.2. Integration of vasculature in spheroid-based TMOCs

As previously discussed, spheroids mimic *in vivo* tumors in terms of shape, high cell density and biochemical *milieu* [75], thus enabling the development of *in vitro* models recapitulating relevant cellular functions [122,123]. Several studies have been conducted to incorporate the vascular network by co-culturing endothelial cells outside [124,125] or inside the tumor spheroid [126–128] under static conditions.

A further advance is represented by the recapitulation of intraluminal flow on engineered tumor vascular networks, as reported in Ref. [75]. The microfluidic platform was characterized by three parallel channels separated by trapezoidal micro-posts. The central channel hosted cancer spheroids, either alone or in combination with fibroblasts and endothelial cells, in a fibrin/collagen matrix, while the two side channels were seeded with HUVECs. During culture, the formation of angiogenetic sprouts was reported, which constructed a perfusable vascular network in the tumor spheroid. Medium perfusion significantly increased cell proliferation and viability compared to the static condition, indicating that the presence of the vasculature ameliorated the supply of nutrients, also affecting the response of cancer cells to anticancer drugs (e.g. paclitaxel).

Sprouting angiogenesis, consisting in the growth of new capillaries emerging from existing ones, is involved in cancer development and invasion of surrounding tissues and it is also fundamental in the metastasic processes. A model for the analysis of sprouted capillaries was proposed to study angiogenesis during the administration of anticancer drugs [129]. Specifically, a perfusable 3D vascularized tumor platform was developed, in which capillaries germinated spontaneously through a hydrogel matrix toward the tumor spheroid. The whole device was made in hydrogel (type I collagen and fibrin) and featured three parallel channels (namely: a central vascular channel lined with HUVECs flanked by a hollow channel and a channel loaded with hLFs, Fig. 5A). A tumor spheroid (A549 cells) was inserted in the hLF channel, and an interstitial flow was generated toward the hollow channel by regulating the height of medium reservoirs, inducing an angiogenic sprouting from the vascular channel toward the hLF channel. Conversely, in the absence of interstitial flow, HUVECs showed no sprouting or preferential migration. The presence of the sprouted capillaries was demonstrated to regulate relevant phenomena including anti-cancer effect of doxorubicin and immune cell transport from the vascular channel to the tumor site.

Most of the above-reported models are based on self-organization processes, which induce the buildup of a perfusable vascular network sensitive to shear stress [130] and cellular interactions [131,132]. However, these models are not suitable to study tissues lacking the ability to induce neovascularization. Furthermore, it must be considered that *in vivo* vascular networks and 3D tissues are in close contact with the ECM, which mediates a uniform gradient of factors to facilitate tissue growth. To overcome these limitations, a microfluidic model was developed enabling the co-culture of tumor spheroids on a pre-formed vascular bed, not necessitating angiogenic factors secreted by the tumor [133]. The device (Fig. 5B) was characterized by a main chamber in which hLFs and HUVECs were cultured in fibrin-collagen gel, flanked by two medium supply channels separated by micro-posts to achieve gel confinement. The main chamber was surmounted by a well for the culture of the tumor spheroid derived by alveolar soft part sarcoma (ASPS) cells. A removable membrane (either polyester or alginate-based) was placed at the bottom of the well to initially separate the spheroid culture chamber from the underlying chamber, where the vascular bed was formed under stimulation from the growth factors secreted by hLFs. Once the membrane was removed, the spheroid contacted the vascular bed, and ASPS cells migration and interaction with the microvasculature could be monitored.

#### 3.2.3. Effect of vascularization in anticancer therapy

As systemically administered chemotherapeutics must overcome the vascular barrier and reach the tumor, endothelial cells can represent an obstacle due to drug absorption, which may result in a weaker tumor response to chemotherapy.

To investigate drug delivery in a vascularized 3D TMOC model [134], a previously validated chip design [135,136] was adapted to the culture of tumor spheroids (Skov3 ovarian and A549 lung tumor cells) within a perfusable microvascular network. Treatment with paclitaxel caused a tumor-induced remodeling of TME and tumor-associated vasculature, and a severe effect on endothelial cells viability and function, besides its cytotoxic effect on cancer cells. Of note, in the TMOC model, paclitaxel effects on tumor cells were dampened compared to simple cancer cell spheroids used as a control, hence underlining the importance of the vasculature and TME recapitulation for predictive drug assessment.

Growing attention has been drawn to mimicking the biochemical signature of the ECM, with the final aim to recapitulate the TME, as in

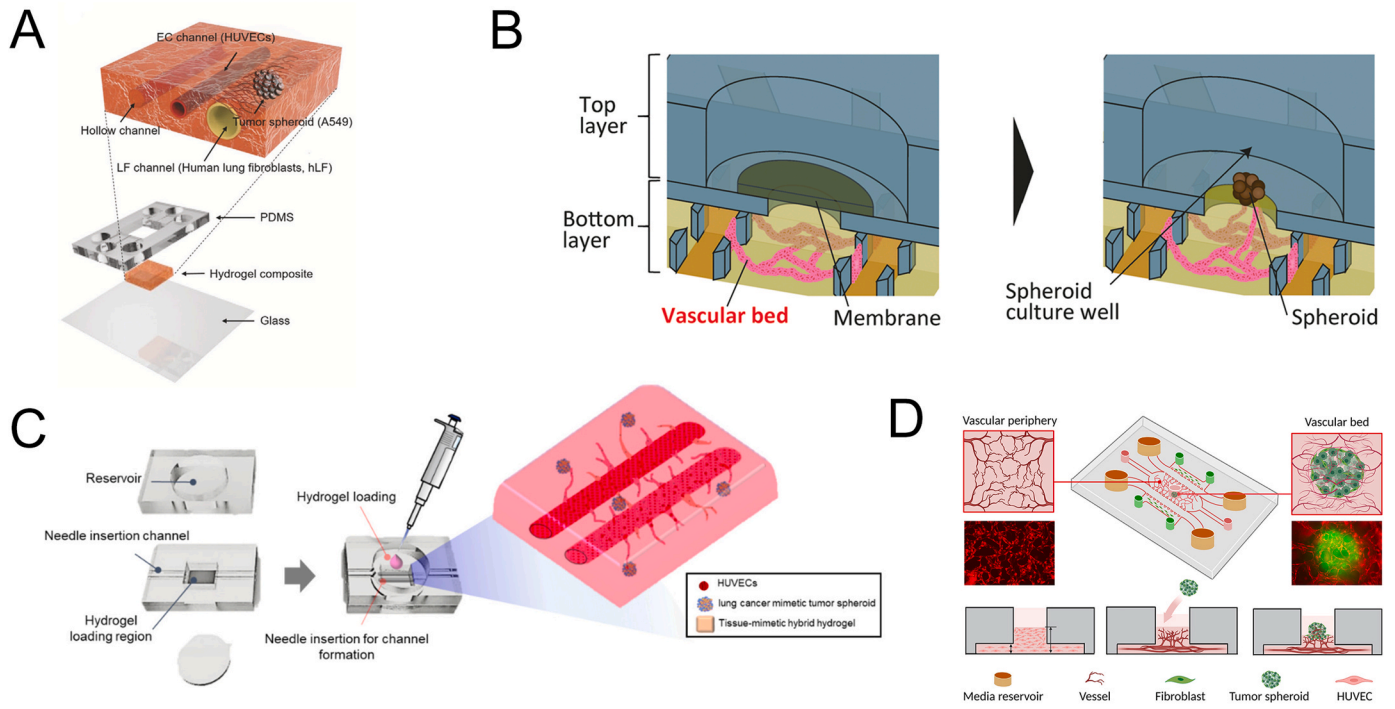


**Fig. 5.** *Microfluidic platforms integrating spheroid-based tumor models with an engineered microvasculature. (A) Representation of a 3D vascularized lung cancer model to study angiogenic sprouting. Adapted with permission from* Ref. [129]. *(B) Schematic design of the microfluidic device for the co-culture of tumor spheroids on a pre-formed vascular bed. Reproduced with permission from* Ref. [133]. *(C) 3D vascularized lung cancer-on-a-chip, with patient-derived tumor spheroids embedded in a lung ECM-derived hydrogel matrix. Reproduced with permission from* Ref. [137]. *(D) Schematic representation of the vascularized esophageal carcinoma spheroid-on-a-chip developed to demonstrate the vasoprotective effect of DMOG. Reproduced with permission from* Ref. [138].

the case of a 3D vascularized on-chip lung cancer model featuring an ECM-derived hydrogel [137]. Spheroids made of A549 cells, HUVECs and hLFs were encapsulated in a hydrogel based on decellularized lung ECM mixed with collagen, to simulate solid-type lung cancer. In addition, two hollow channels were incorporated in the hydrogel and seeded with HUVECs to simulate a capillary network (Fig. 5C). By tuning the mechanical and biochemical properties of the hydrogel, an improvement in cell viability and in angiogenesis was observed; this confirmed that the decellularized pulmonary ECM, thanks to the presence of pro-angiogenic growth factors and cytokines, could initiate vascularization and represented an ideal tool for imitating the natural microenvironment. Moreover, the proposed 3D vascularized model was treated with doxorubicin, showing markedly dose-dependent effects of the drug compared to non-vascularized 2D and 3D cell cultures. Thus, the uptake of doxorubicin occurred in a similar way to native tumors, with a significant dose-dependent variation of its cytotoxic effects on endothelial cells, which undergo apoptosis at high doses of doxorubicin.

What distinguishes tumors from normal tissues is the type of abnormal vascularization characterized by permeable blood vessels that lead to hypoxia, nutrient depletion and elevated interstitial pressure [138]. The last factor reverses the pressure gradients normally present in the tissue and ultimately prevents the penetration of molecules, including chemotherapeutic agents. In these conditions, the therapeutic efficacy is reduced, favoring the progression of the disease. In recent years, *in vitro* studies have demonstrated that dimethyloxalylglycine (DMOG), an inhibitor of prolyl hydroxylase that regulates hypoxia-inducible factors, possesses angiogenic properties capable of normalizing blood vessels leading to an increase in perfusion, oxygen, and drug distribution [139]. In this context, an on-chip, perfusable and vascularized esophageal carcinoma cell-derived tumor spheroid model was developed to demonstrate the vasoprotective and angiogenic effects of DMOG [138]. The microfluidic device featured a set of parallel channels separated by micro-pillar arrays (Fig. 5D). In the central channel, HUVEC in fibrin gel were introduced as the vascular bed. Vascular maturation was enhanced by the presence of fibroblasts in the lateral channels. Tumor spheroids were then inoculated in the pre-formed vascular bed. Exposure to DMOG resulted in increased drug efficacy and apoptosis of cancer cells and protected normal blood vessels from the damage caused by chemotherapy drugs such as paclitaxel and cisplatin.

## 4. Toward multi-organ models integrating TMOCs

One recent trend in the field of TMOCs regards their integration into multi-organ microphysiological systems (multi-OoC), aiming at interfacing multiple organs/tissues in a closed loop [140,141]. This approach has allowed scientists to better investigate the crosstalk between tumor metastasis and distant organs and to elucidate the (side) effects of chemotherapies on a more systemic perspective [44].

One of the first attempts to address organ specificity of tumor metastases is represented by the interconnection of a colon cancer model with a liver model, successfully tracking tumor cells homing to the target organ [142]. A more complex approach is represented by the work of Aleman et al. [143], who investigated the metastatic preference of colorectal cancer through a multi-chamber device hosting the tumor model (HTC116 colorectal cancer cells) connected to downstream chambers hosting liver, lung and endothelial constructs. Tumor cells showed a metastatic preference for the liver and lung constructs, in good agreement with clinical evidence. A similar approach was followed in the case of lung cancer, where the metastatic preference was evaluated using bone, brain, and liver as target organs [144]. Of note, the authors implemented a fully developed TMOC model, including epithelial cells, lung cancer cells, stromal fibroblasts, mononuclear cells, and microvascular endothelium, to fully recapitulate the TME (Fig. 6A).

Another primary application of the multi-OoC approach involves the study of anticancer therapies and biological processes driving tumor resistance to treatments. As the cytotoxic effects of anticancer drugs are not limited to cancer cells, but are known to generate a cascade of inter-

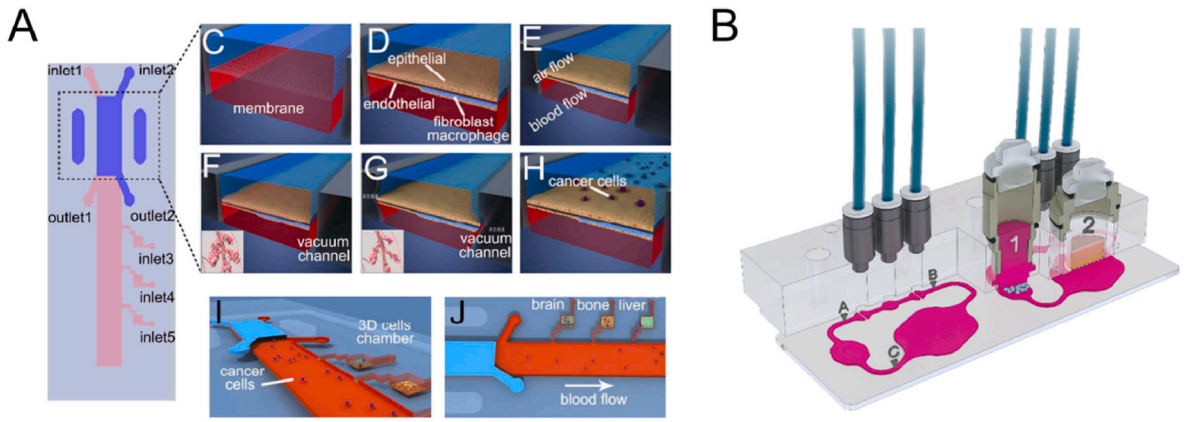


**Fig. 6.** *Multi-organ models. (A) Schematic representation of a multi-organ microfluidic chip, which includes an upstream "lung organ" and three downstream "distant organs". Adapted with permission from* Ref. [144]*; (B) Schematic representation of the microfluidic device integrating a lung cancer model with a full thickness skin equivalent; the cross-section on the right shows the tumor (1) and skin (2) compartments, respectively, while the cross-section on the left shows the fluidic connection of the two models. Adapted with permission from* Ref. [145].

organ events, multi-OoC platforms have proved suitable to address these aspects. By fluidically coupling different tissues/organs, the elucidation of phenomena involving drug pharmacokinetics and direct/indirect effects in other organs can be investigated.

The integration of a lung cancer model with a full-thickness skin equivalent has been proposed as a model to assess the adverse effects of an anti-EGFR antibody (cetuximab) [145] (Fig. 6B). Beside the desired pro-apoptotic effects on the tumor micromass, the authors reported crucial inhibition of the physiological skin turnover, in agreement with clinical evidence.

The known cardiotoxic effects of doxorubicin have been modeled using a multi-OoC featuring the interconnection of a liver cancer model with a human healthy heart cells under closed loop perfusion achieved via an on-chip integrated micropump [146]. The model successfully recapitulated the accumulation in heart cells of the highly cardiotoxic metabolite doxorubicinol. These results were confirmed in a similar study on a liver-cancer/heart model [147] highlighting how microfluidic perfusion was associated with increased cardiotoxicity compared to control static cultures.

Significant effects of perfusion conditions on drug sensitivity were also reported employing a multi-OoC integrating human ovarian tumor and liver OoCs, measuring differential drug sensitivity levels between dynamic multi-organ settings and static co-culture controls [148].

The previous findings evidence the key role of mass transport phenomena in multi-OoC implementation, mandating for a rigorous design and simulation step to mimic *in-vivo*-like conditions.

Multi-OoCs have also shown the potential to study the effectiveness of anticancer drugs in the form of prodrugs. A multi-OoC platform was proposed to investigate the hepatic metabolism of the anticancer prodrug capecitabine (CAP) and its metabolite 5-fluorouracyl (5-FU) [149]. The chip, featuring a liver and a cancer compartment, was used to demonstrate the antiblastic effect of 5-FU following biotransformation of CAP by liver cells. The model was further expanded to a 4-organ system, achieving the direct measurement of the chemotherapy effect on different tissues.

With a similar aim, the anticancer effect of cyclophosphamide was evaluated against primary and metastatic oral squamous cell carcinoma in the presence or absence of liver biotransformation [150]. An original modular design (named Tetris-Like, TILE) was conceived, achieving effective and self-aligning on-the-fly fluidic connection of several modular units and easing the establishment of different multi-organ configurations. Similar research studies involving multi-organ reflexes of prodrug metabolism have been reported in the case of glioblastoma [151] and lung cancer [152,153].

## 5. Summary and future perspective

With the growing push of regulatory agencies (e.g., FDA Modernization Act 2.0 [154]) to advance the development of alternative methods which can replace, reduce and refine (3Rs) animal testing in the pharma industry, we are witnessing the ascent of microphysiological systems as a new avenue for cancer research. Leveraging the peculiar aspects of 2D/3D cell culture in microfluidic regimes, these systems enable more accurate control over spatio-temporal gradients of biochemical factors and precise cell positioning and confinement, resulting in more robust and reproducible culture settings. Over the past decade, significant advances have been reported concerning the recapitulation of human-like tumor niche on-chip by co-culturing tumor cells in combination with other components of the TME, including stromal cells, immune cells, and endothelial cells. This has been accompanied by the development of tissue-specific ECM-like matrices for the 3D culture of cells either laden in hydrogels or in the form of multicellular tumor spheroids. 3D tumor spheroids effectively reproduce the cell-cell and cell-ECM interactions occurring between the tumor and the surrounding microenvironment. For this reason, they are increasingly being used for the evaluation of novel anticancer therapies, including the study and *in vitro* validation of adoptive cell therapies, such as those based on TCR-T and CAR-T cells. In this regard, the integration of the vascular component represents a key aspect determining the predictivity of TMOC models, as the dynamic interactions occurring between tumor and vasculature play a major role in orchestrating cancer progression and response to drugs.

The most recent trend in TMOCs research regards their integration into more sophisticated multi-organ platforms (multi-OoCs), tailored for the study of metastatic processes—which directly link the primary tumor with distant organs—and for the elucidation of the systemic effects of anticancer drugs. Recent findings underline the great potential of multi-OoCs as the next step toward more robust and predictive platforms. In this regard, we envisage the leading role of induced pluripotent stem cell (iPSC) technology, which is expected to support the development of organ models with increasing pathophysiological relevance to be interconnected with TMOCs. We also expect the future generation of multi-OoC systems to be endowed with on-board biosensors for *in situ* real-time readout of cell biochemical/biological responses. Robotics and Artificial Intelligence are also expected to play a leading role in the automation of OoC operation and data analysis, hence improving the throughput of these platforms.

## CRediT authorship contribution statement

**S.M. Giannitelli:** Writing – original draft, Writing – review & editing. **V. Peluzzi:** Writing – original draft, Writing – review & editing. **S. Raniolo:** Writing – original draft. **G. Roscilli:** Writing – review & editing. **M. Trombetta:** Funding acquisition, Writing – original draft, Writing – review & editing. **P. Mozetic:** Writing – review & editing. **A. Rainer:** Supervision, Writing – original draft, Writing – review & editing.

## Declaration of competing interest

The authors declare that they have no known competing financial interests or personal relationships that could have appeared to influence the work reported in this paper.

## Data availability

No data was used for the research described in the article.

## Acknowledgment

This work is funded by the European Union - Next Generation EU - NRRP M4.C2 - Investment 1.5 Establishing and strengthening of Innovation Ecosystems for sustainability (Project n. ECS00000024 Rome Technopole). P.M. acknowledges the “National Center for Gene Therapy and Drugs based on RNA Technology” (CN00000041 CN3 RNA), funded by the European Union - Next Generation EU - NRRP M4.C2 - Investment 1.4.

## References

[1] A. Sontheimer-Phelps, B.A. Hassell, D.E. Ingber, Modelling cancer in microfluidic human organs-on-chips, Nat. Rev. Cancer 19 (2019) 65–81, https://doi.org/10.1038/s41568-018-0104-6.
[2] K.E. de Visser, J.A. Joyce, The evolving tumor microenvironment: from cancer initiation to metastatic outgrowth, Cancer Cell 41 (2023) 374–403, https://doi.org/10.1016/j.ccell.2023.02.016.
[3] R. Baghban, L. Roshangar, R. Jahanban-Esfahlan, K. Seidi, A. Ebrahimi-Kalan, M. Jaymand, S. Kolahian, T. Javaheri, P. Zare, Tumor microenvironment complexity and therapeutic implications at a glance, Cell Commun. Signal. 18 (2020) 1–19, https://doi.org/10.1186/s12964-020-0530-4.
[4] Y. Xiao, D. Yu, Tumor microenvironment as a therapeutic target in cancer, Pharmacol. Ther. 221 (2021) 107753, https://doi.org/10.1016/j.pharmthera.2020.107753.
[5] L. Bejarano, M.J.C. Jordão, J.A. Joyce, Therapeutic targeting of the tumor microenvironment, Cancer Discov. 11 (2021) 933–959, https://doi.org/10.1158/2159-8290.CD-20-1808.
[6] E.J. Lee, Z.L. Krassin, H.E. Abaci, G.J. Mahler, M.B. Esch, Pumped and pumpless microphysiological systems to study (nano)therapeutics, Rev. Nanomedicine Nanobiotechnology. 15 (2023) e1911, https://doi.org/10.1002/wnan.1911. Wiley Interdiscip.
[7] N. Dhiman, P. Kingshott, H. Sumer, C.S. Sharma, S.N. Rath, On-chip anticancer drug screening–recent progress in microfluidic platforms to address challenges in chemotherapy, Biosens. Bioelectron 137 (2019) 236–254, https://doi.org/10.1016/j.bios.2019.02.070.
[8] S.M. Giannitelli, M. Costantini, F. Basoli, M. Trombetta, A. Rainer, Electrospinning and microfluidics: an integrated approach for tissue engineering and cancer, in: V. Guarino, L.B.T.-E.T.( EFDTs, B. for, M.D. Ambrosio (Eds.), Electrofluidodynamic Technol. Biomater. Med. Devices Princ. Adv., Woodhead Publishing, 2018, pp. 139–155, https://doi.org/10.1016/B978-0-08-101745-6.00008-6.
[9] J.M. Ayuso, K.-Y. Park, M. Virumbrales-Muñoz, D.J. Beebe, Toward improved in vitro models of human cancer, APL Bioeng. 5 (2021) 10902, https://doi.org/10.1063/5.0026857.
[10] C. Li, J.B. Holman, Z. Shi, B. Qiu, W. Ding, On-chip modeling of tumor evolution: advances, challenges and opportunities, Mater. Today Bio. 21 (2023) 100724, https://doi.org/10.1016/j.mtbio.2023.100724.
[11] Y. Zhao, E.Y. Wang, F.B.L. Lai, K. Cheung, M. Radisic, Organs-on-a-chip: a union of tissue engineering and microfabrication, Trends Biotechnol. 41 (2023) 410–424, https://doi.org/10.1016/j.tibtech.2022.12.018.
[12] K. Wang, K. Man, J. Liu, Y. Liu, Q. Chen, Y. Zhou, Y. Yang, Microphysiological systems: design, fabrication, and applications, ACS Biomater. Sci. Eng. 6 (2020) 3231–3257, https://doi.org/10.1021/acsbiomaterials.9b01667.
[13] L.A. Low, C. Mummery, B.R. Berridge, C.P. Austin, D.A. Tagle, Organs-on-chips: into the next decade, Nat. Rev. Drug Discov. 20 (2021) 345–361, https://doi.org/10.1038/s41573-020-0079-3.
[14] E. Ferrari, C. Palma, S. Vesentini, P. Occhetta, M. Rasponi, Integrating biosensors in organs-on-chip devices: a perspective on current strategies to monitor microphysiological systems, Biosensors 10 (2020) 110, https://doi.org/10.3390/bios10090110.
[15] M. Gori, S.M. Giannitelli, A. Zancla, P. Mozetic, M. Trombetta, N. Merendino, A. Rainer, Quercetin and hydroxytyrosol as modulators of hepatic steatosis: a NAFLD-on-a-chip study, Biotechnol. Bioeng. 118 (2021) 142–152, https://doi.org/10.1002/bit.27557.
[16] A. Gizzi, S.M. Giannitelli, M. Trombetta, C. Cherubini, S. Filippi, A. De Ninno, L. Businaro, A. Gerardino, A. Rainer, Computationally Informed design of a multi-axial actuated microfluidic chip device, Sci. Rep. 7 (2017) 1–11, https://doi.org/10.1038/s41598-017-05237-9.
[17] A.R. Perestrelo, A.C.P. Águas, A. Rainer, G. Forte, Microfluidic organ/body-on-a-chip devices at the convergence of biology and microengineering, Sensors 15 (2015) 31142–31170, https://doi.org/10.3390/s151229848.
[18] Y. Ando, C. Mariano, K. Shen, Engineered in vitro tumor models for cell-based immunotherapy, Acta Biomater. 132 (2021) 345–359, https://doi.org/10.1016/j.actbio.2021.03.076.
[19] D.E. Ingber, Reverse engineering human pathophysiology with organs-on-chips, Cell 164 (2016) 1105–1109, https://doi.org/10.1016/j.cell.2016.02.049.
[20] L.K. Chin, C.-H. Lee, B.-C. Chen, Imaging live cells at high spatiotemporal resolution for lab-on-a-chip applications, Lab Chip 16 (2016) 2014–2024, https://doi.org/10.1039/c5lc01556a.
[21] A. Marsano, C. Conficconi, M. Lemme, P. Occhetta, E. Gaudiello, E. Votta, G. Cerino, A. Redaelli, M. Rasponi, Beating heart on a chip: a novel microfluidic platform to generate functional 3D cardiac microtissues, Lab Chip 16 (2016) 599–610, https://doi.org/10.1039/c5lc01356a.
[22] H.J. Kim, D. Huh, G. Hamilton, D.E. Ingber, Human gut-on-a-chip inhabited by microbial flora that experiences intestinal peristalsis-like motions and flow, Lab Chip 12 (2012) 2165–2174, https://doi.org/10.1039/C2LC40074J.
[23] S.B. Campbell, Q. Wu, J. Yazbeck, C. Liu, S. Okhovatian, M. Radisic, Beyond polydimethylsiloxane: alternative materials for fabrication of organ-on-a-chip devices and microphysiological systems, ACS Biomater. Sci. Eng. 7 (2021) 2880–2899, https://doi.org/10.1021/acsbiomaterials.0c00640.
[24] L.J.Y. Ong, A. Islam, R. Dasgupta, N.G. Iyer, H.L. Leo, Y.C. Toh, A 3D printed microfluidic perfusion device for multicellular spheroid cultures, Biofabrication 9 (2017) 45005, https://doi.org/10.1088/1758-5090/aa8858.
[25] C.M. Leung, P. De Haan, K. Ronaldson-Bouchard, G.-A. Kim, J. Ko, H.S. Rho, Z. Chen, P. Habibovic, N.L. Jeon, S. Takayama, A guide to the organ-on-a-chip, Nat. Rev. Methods Prim. 2 (2022) 33, https://doi.org/10.1038/s43586-022-00118-6.
[26] M. Abulaiti, Y. Yalikun, K. Murata, A. Sato, M.M. Sami, Y. Sasaki, Y. Fujiwara, K. Minatoya, Y. Shiba, Y. Tanaka, Establishment of a heart-on-a-chip microdevice based on human iPS cells for the evaluation of human heart tissue function, Sci. Rep. 10 (2020) 19201, https://doi.org/10.1038/s41598-020-76062-w.
[27] C. Shen, H. Yang, W. She, Q. Meng, A microfluidic lung-on-a-chip based on biomimetic hydrogel membrane, Biotechnol. Bioeng. (2023), https://doi.org/10.1002/bit.28426.
[28] J. Yang, Y. Hirai, K. Iida, S. Ito, M. Trumm, S. Terada, R. Sakai, T. Tsuchiya, O. Tabata, K. Kamei, Integrated-gut-liver-on-a-chip platform as an in vitro human model of non-alcoholic fatty liver disease, Commun. Biol. 6 (2023) 310, https://doi.org/10.1038/s42003-023-04710-8.
[29] E.M. Vedula, J.L. Alonso, M.A. Arnaout, J.L. Charest, A microfluidic renal proximal tubule with active reabsorptive function, PLoS One 12 (2017) e0184330, https://doi.org/10.1371/journal.pone.0184330.
[30] Y. Fan, C. Xu, N. Deng, Z. Gao, Z. Jiang, X. Li, Y. Zhou, H. Pei, L. Li, B. Tang, Understanding drug nanocarrier and blood–brain barrier interaction based on a microfluidic microphysiological model, Lab Chip 23 (2023) 1935–1944, https://doi.org/10.1039/D2LC01077A.
[31] C. He, F. Lu, Y. Liu, Y. Lei, X. Wang, N. Tang, Emergent trends in organ-on-a-chip applications for investigating metastasis within tumor microenvironment: a comprehensive bibliometric analysis, Heliyon 10 (2024) e23504, https://doi.org/10.1016/j.heliyon.2023.e23504.
[32] B. Subia, U.R. Dahiya, S. Mishra, J. Ayache, G.V. Casquillas, D. Caballero, R. L. Reis, S.C. Kundu, Breast tumor-on-chip models: from disease modeling to personalized drug screening, J. Contr. Release 331 (2021) 103–120, https://doi.org/10.1016/j.jconrel.2020.12.057.
[33] C. Shao, Y. Yu, X. Lei, J. Cao, Y. Zhao, F. Ye, Organ-on-a-chip for dynamic tumor drug resistance investigation, Chem. Eng. J. 460 (2023) 141739, https://doi.org/10.1016/j.cej.2023.141739.
[34] Z. Yang, Z. Zhou, T. Si, Z. Zhou, L. Zhou, Y.R. Chin, L. Zhang, X. Guan, M. Yang, High throughput confined migration microfluidic device for drug screening, Small 19 (2023) 2207194, https://doi.org/10.1002/smll.202207194.
[35] J. Ro, J. Kim, Y.K. Cho, Recent advances in spheroid-based microfluidic models to mimic the tumour microenvironment, Analyst (10) (2022) 147, https://doi.org/10.1039/d2an00172a.
[36] C. Jensen, Y. Teng, Is it time to start transitioning from 2D to 3D cell culture? Front. Mol. Biosci. 7 (2020) 33, https://doi.org/10.3389/fmolb.2020.00033.
[37] J. Rouwkema, A. Khademhosseini, Vascularization and angiogenesis in tissue engineering: beyond creating static networks, Trends Biotechnol. 34 (2016) 733–745, https://doi.org/10.1016/j.tibtech.2016.03.002.
[38] X. Liu, J. Fang, S. Huang, X. Wu, X. Xie, J. Wang, F. Liu, M. Zhang, Z. Peng, N. Hu, Tumor-on-a-chip: from bioinspired design to biomedical application,

Microsystems Nanoeng 7 (2021) 1–23, https://doi.org/10.1038/s41378-021-00277-8.
[39] A.A. Khalili, M.R. Ahmad, A Review of cell adhesion studies for biomedical and biological applications, Int. J. Mol. Sci. 16 (2015) 18149–18184, https://doi.org/10.3390/ijms160818149.
[40] G. Lamberti, B. Prabhakarpandian, C. Garson, A. Smith, K. Pant, B. Wang, M. F. Kiani, Bioinspired microfluidic assay for in vitro modeling of leukocyte–endothelium interactions, Anal. Chem. 86 (2014) 8344–8351, https://doi.org/10.1021/ac5018716.
[41] S. Mi, Z. Du, Y. Xu, Z. Wu, X. Qian, M. Zhang, W. Sun, Microfluidic co-culture system for cancer migratory analysis and anti-metastatic drugs screening, Sci. Rep. 6 (2016) 1–11, https://doi.org/10.1038/srep35544.
[42] R. Kalluri, The biology and function of fibroblasts in cancer, Nat. Rev. Cancer 16 (2016) 582–598, https://doi.org/10.1038/nrc.2016.73.
[43] A.E. Karnoub, A.B. Dash, A.P. Vo, A. Sullivan, M.W. Brooks, G.W. Bell, A. L. Richardson, K. Polyak, R. Tubo, R.A. Weinberg, Mesenchymal stem cells within tumour stroma promote breast cancer metastasis, Nature 449 (2007) 557–563, https://doi.org/10.1038/nature06188.
[44] G. Imparato, F. Urciuolo, C. Mazio, P.A. Netti, Capturing the spatial and temporal dynamics of tumor stroma for on-chip optimization of microenvironmental targeting nanomedicine, Lab Chip 23 (2023) 25–43, https://doi.org/10.1039/D2LC00611A.
[45] M.A. Lakins, E. Ghorani, H. Munir, C.P. Martins, J.D. Shields, Cancer-associated fibroblasts induce antigen-specific deletion of CD8 + T Cells to protect tumour cells, Nat. Commun. 9 (2018) 1–9, https://doi.org/10.1038/s41467-018-03347-0.
[46] M. Li, X. Sun, X. Kuang, Y. Liao, H. Li, D. Luo, Mesenchymal stem cells suppress CD8+ T cell-mediated activation by suppressing natural killer group 2, member D protein receptor expression and secretion of prostaglandin E2, indoleamine 2, 3-dioxygenase and transforming growth factor-β, Clin. Exp. Immunol. 178 (2014) 516–524, https://doi.org/10.1111/cei.12423.
[47] M.P. V Shekhar, R. Pauley, G. Heppner, Host microenvironment in breast cancer development: extracellular matrix–stromal cell contribution to neoplastic phenotype of epithelial cells in the breast, Breast Cancer Res. 5 (2003) 130, https://doi.org/10.1186/bcr580.
[48] D.D. Truong, A. Kratz, J.G. Park, E.S. Barrientos, H. Saini, T. Nguyen, B. Pockaj, G. Mouneimne, J. LaBaer, M. Nikkhah, A human organotypic microfluidic tumor model permits investigation of the interplay between patient-derived fibroblasts and breast cancer cells, Cancer Res. 79 (2019) 3139–3151, https://doi.org/10.1158/0008-5472.CAN-18-2293.
[49] D. Truong, J. Puleo, A. Llave, G. Mouneimne, R.D. Kamm, M. Nikkhah, Breast cancer cell invasion into a three dimensional tumor-stroma microenvironment, Sci. Rep. 6 (2016) 1–18, https://doi.org/10.1038/srep34094.
[50] N. Peela, E.S. Barrientos, D. Truong, G. Mouneimne, M. Nikkhah, Effect of suberoylanilide hydroxamic acid (SAHA) on breast cancer cells within a tumor-stroma microfluidic model, Integr. Biol. 9 (2017) 988–999, https://doi.org/10.1039/c7ib00180k.
[51] F. Gioiella, F. Urciuolo, G. Imparato, V. Brancato, P.A. Netti, An engineered breast cancer model on a chip to replicate ECM-activation in vitro during tumor progression, Adv. Healthc. Mater. 5 (2016) 3074–3084, https://doi.org/10.1002/adhm.201600772.
[52] X. Lei, Y. Lei, J.K. Li, W.X. Du, R.G. Li, J. Yang, J. Li, F. Li, H.B. Tan, Immune cells within the tumor microenvironment: biological functions and roles in cancer immunotherapy, Cancer Lett. 470 (2020) 126–133, https://doi.org/10.1016/j.canlet.2019.11.009.
[53] Y. Ino, R. Yamazaki-Itoh, K. Shimada, M. Iwasaki, T. Kosuge, Y. Kanai, N. Hiraoka, Immune cell infiltration as an indicator of the immune microenvironment of pancreatic cancer, Br. J. Cancer 108 (2013) 914–923, https://doi.org/10.1038/bjc.2013.32.
[54] Q. Xu, S. Chen, Y. Hu, W. Huang, Landscape of immune microenvironment under immune cell infiltration pattern in breast cancer, Front. Immunol. 12 (2021) 711433, https://doi.org/10.3389/fimmu.2021.711433.
[55] R. Zhou, J. Zhang, D. Zeng, H. Sun, X. Rong, M. Shi, J. Bin, Y. Liao, W. Liao, Immune cell infiltration as a biomarker for the diagnosis and prognosis of stage I-III colon cancer, Cancer Immunol. Immunother. 68 (2019) 433–442, https://doi.org/10.1007/s00262-018-2289-7.
[56] S.C. Chen, P.C. Wu, C.Y. Wang, P.L. Kuo, Evaluation of cytotoxic T lymphocyte-mediated anticancer response against tumor interstitium-simulating physical barriers, Sci. Rep. 10 (2020) 1–13, https://doi.org/10.1038/s41598-020-70694-8.
[57] E. Vacchelli, Y. Ma, E.E. Baracco, A. Sistigu, D.P. Enot, F. Pietrocola, H. Yang, S. Adjemian, K. Chaba, M. Semeraro, M. Signore, A. De Ninno, V. Lucarini, F. Peschiaroli, L. Businaro, A. Gerardino, G. Manic, T. Ulas, P. Günther, J. L. Schultze, O. Kepp, G. Stoll, C. Lefebvre, C. Mulot, F. Castoldi, S. Rusakiewicz, S. Ladoire, L. Apetoh, J.M.B.S. Pedro, M. Lucattelli, C. Delarasse, V. Boige, M. Ducreux, S. Delaloge, C. Borg, F. André, G. Schiavoni, I. Vitale, P. Laurent-Puig, F. Mattei, L. Zitvogel, G. Kroemer, Chemotherapy-induced antitumor immunity requires formyl peptide receptor 1, Science 350 (80-) (2015) 972–978, https://doi.org/10.1126/science.aad0779.
[58] V. Lucarini, C. Buccione, G. Zicchedda, F. Peschiaroli, P. Sestili, R. Puglisi, G. Mattia, C. Zanetti, I. Parolini, L. Bracci, I. Macchia, A. Rossi, M.T. D'Urso, D. Macchia, M. Spada, A. De Ninno, A. Gerardino, P. Mozetic, M. Trombetta, A. Rainer, L. Businaro, G. Schiavoni, F. Mattei, Combining type I interferons and 5-aza-2′-deoxycitidine to improve anti-tumor response against melanoma, J. Invest. Dermatol. 137 (2017) 159–169, https://doi.org/10.1016/j.jid.2016.08.024.
[59] S.W.L. Lee, G. Adriani, E. Ceccarello, A. Pavesi, A.T. Tan, A. Bertoletti, R. D. Kamm, S.C. Wong, Corrigendum: characterizing the role of monocytes in T cell cancer immunotherapy using a 3D microfluidic model, Front. Immunol. 9 (2018) 416, https://doi.org/10.3389/fimmu.2018.01719. Front Immunol, 9, (2018), (416)] DOI: 10.3389/fimmu.2018.00416.
[60] A. Pavesi, A.T. Tan, S. Koh, A. Chia, M. Colombo, E. Antonecchia, C. Miccolis, E. Ceccarello, G. Adriani, M.T. Raimondi, R.D. Kamm, A. Bertoletti, A 3D microfluidic model for preclinical evaluation of TCR-engineered T cells against solid tumors, JCI Insight 2 (2017), https://doi.org/10.1172/jci.insight.89762.
[61] G. Chen, K. Wu, H. Li, D. Xia, T. He, Role of hypoxia in the tumor microenvironment and targeted therapy, Front. Oncol. 12 (2022) 961637, https://doi.org/10.3389/fonc.2022.961637.
[62] V. Nizet, R.S. Johnson, Interdependence of hypoxic and innate immune responses, Nat. Rev. Immunol. 9 (2009) 609–617, https://doi.org/10.1038/nri2607.
[63] I.B. Barsoum, C.A. Smallwood, D.R. Siemens, C.H. Graham, A mechanism of hypoxia-mediated escape from adaptive immunity in cancer cells, Cancer Res. 74 (2014) 665–674, https://doi.org/10.1158/0008-5472.CAN-13-0992.
[64] C.S. Curran, P.J. Keely, Breast tumor and stromal cell responses to TGF-β and hypoxia in matrix deposition, Matrix Biol. 32 (2013) 95–105, https://doi.org/10.1016/j.matbio.2012.11.016.
[65] C. Furuta, T. Miyamoto, T. Takagi, Y. Noguchi, J. Kaneko, S. Itoh, T. Watanabe, F. Itoh, Transforming growth factor-β signaling enhancement by long-term exposure to hypoxia in a tumor microenvironment composed of Lewis lung carcinoma cells, Cancer Sci. 106 (2015) 1524–1533, https://doi.org/10.1111/cas.12773.
[66] P. Vaupel, A. Mayer, Hypoxia-driven adenosine accumulation: a crucial microenvironmental factor promoting tumor progression, in: Adv. Exp. Med. Biol., Springer, 2016, p. 177, https://doi.org/10.1007/978-1-4939-3023-4_22.
[67] J. Blay, T.D. White, D.W. Hoskin, The extracellular fluid of solid carcinomas contains immunosuppressive concentrations of adenosine, Cancer Res. 57 (1997) 2602–2605.
[68] M.V. Sitkovsky, A. Ohta, The "danger" sensors that STOP the immune response: the A2 adenosine receptors? Trends Immunol. 26 (2005) 299–304, https://doi.org/10.1016/j.it.2005.04.004.
[69] Y. Ando, E.L. Siegler, H.P. Ta, G.E. Cinay, H. Zhou, K.A. Gorrell, H. Au, B. M. Jarvis, P. Wang, K. Shen, Evaluating CAR-T cell therapy in a hypoxic 3D tumor model, Adv. Healthc. Mater. 8 (2019) 1900001, https://doi.org/10.1002/adhm.201900001.
[70] Y. Ando, H.P. Ta, D.P. Yen, S.S. Lee, S. Raola, K. Shen, A microdevice platform recapitulating hypoxic tumor microenvironments, Sci. Rep. 7 (2017) 1–12, https://doi.org/10.1038/s41598-017-15583-3.
[71] S. Parlato, G. Grisanti, G. Sinibaldi, G. Peruzzi, C.M. Casciola, L. Gabriele, Tumor-on-a-chip platforms to study cancer-immune system crosstalk in the era of immunotherapy, Lab Chip 21 (2021) 234–253, https://doi.org/10.1039/d0lc00799d.
[72] X. Wang, Q. Sun, J. Pei, Microfluidic-based 3D engineered microvascular networks and their applications in vascularized microtumor models, Micromachines 9 (2018) 493, https://doi.org/10.3390/mi9100493.
[73] K.L. Fabian, W.J. Storkus, Immunotherapeutic targeting of tumor-associated blood vessels, Adv. Exp. Med. Biol. 1036 (2017) 191–211, https://doi.org/10.1007/978-3-319-67577-0_13.
[74] M.B. Schaaf, A.D. Garg, P. Agostinis, Defining the role of the tumor vasculature in antitumor immunity and immunotherapy article, Cell Death Dis. 9 (2018) 115, https://doi.org/10.1038/s41419-017-0061-0.
[75] Y. Nashimoto, R. Okada, S. Hanada, Y. Arima, K. Nishiyama, T. Miura, R. Yokokawa, Vascularized cancer on a chip: the effect of perfusion on growth and drug delivery of tumor spheroid, Biomaterials 229 (2020) 119547, https://doi.org/10.1016/j.biomaterials.2019.119547.
[76] S. Rajput, P. Kumar Sharma, R. Malviya, Fluid mechanics in circulating tumour cells: role in metastasis and treatment strategies, Med. Drug Discov 18 (2023) 100158, https://doi.org/10.1016/j.medidd.2023.100158.
[77] X. Li, Y. Li, W. Lu, M. Chen, W. Ye, D. Zhang, The tumor vessel targeting strategy: a double-edged sword in tumor metastasis, Cells 8 (2019) 1602, https://doi.org/10.3390/cells8121602.
[78] A.D. Castiaux, D.M. Spence, R.S. Martin, Review of 3D cell culture with analysis in microfluidic systems, Anal. Methods 11 (2019) 4220–4232, https://doi.org/10.1039/c9ay01328h.
[79] E. Huynh, G. Zheng, Cancer nanomedicine: addressing the dark side of the enhanced permeability and retention effect, Nanomedicine 10 (2015) 1993–1995, https://doi.org/10.2217/nnm.15.86.
[80] F. Danhier, O. Feron, V. Préat, To exploit the tumor microenvironment: passive and active tumor targeting of nanocarriers for anti-cancer drug delivery, J. Contr. Release 148 (2010) 135–146, https://doi.org/10.1016/j.jconrel.2010.08.027.
[81] A. Sobrino, D.T.T. Phan, R. Datta, X. Wang, S.J. Hachey, M. Romero-López, E. Gratton, A.P. Lee, S.C. George, C.C.W. Hughes, 3D microtumors in vitro supported by perfused vascular networks, Sci. Rep. 6 (2016) 1–11, https://doi.org/10.1038/srep31589.
[82] S. Wang, S. Mao, M. Li, H.F. Li, J.M. Lin, Near-physiological microenvironment simulation on chip to evaluate drug resistance of different loci in tumour mass, Talanta 191 (2019) 67–73, https://doi.org/10.1016/j.talanta.2018.08.016.
[83] A. Ozcelikkale, K. Shin, V. Noe-Kim, B.D. Elzey, Z. Dong, J.-T. Zhang, K. Kim, I. C. Kwon, K. Park, B. Han, Differential response to doxorubicin in breast cancer subtypes simulated by a microfluidic tumor model, J. Contr. Release 266 (2017) 129–139, https://doi.org/10.1016/j.jconrel.2017.09.024.
[84] D. Truong, R. Fiorelli, E.S. Barrientos, E.L. Melendez, N. Sanai, S. Mehta, M. Nikkhah, A three-dimensional (3D) organotypic microfluidic model for glioma

stem cells – vascular interactions, Biomaterials 198 (2019) 63–77, https://doi.org/10.1016/j.biomaterials.2018.07.048.
[85] S. Lee, S. Kim, D.J. Koo, J. Yu, H. Cho, H. Lee, J.M. Song, S.Y. Kim, D.H. Min, N. L. Jeon, 3D microfluidic platform and tumor vascular mapping for evaluating anti-angiogenic RNAi-based nanomedicine, ACS Nano 15 (2021) 338–350, https://doi.org/10.1021/acsnano.0c05110.
[86] S. Kim, M. Chung, J. Ahn, S. Lee, N.L. Jeon, Interstitial flow regulates the angiogenic response and phenotype of endothelial cells in a 3D culture model, Lab Chip 16 (2016) 4189–4199, https://doi.org/10.1039/c6lc00910g.
[87] I.M. Gonçalves, V. Carvalho, R.O. Rodrigues, D. Pinho, S.F.C.F. Teixeira, A. Moita, T. Hori, H. Kaji, R. Lima, G. Minas, Organ-on-a-Chip platforms for drug screening and delivery in tumor cells: a systematic review, Cancers 14 (2022) 935, https://doi.org/10.3390/cancers14040935.
[88] A. Hasan, A. Paul, N.E. Vrana, X. Zhao, A. Memic, Y.S. Hwang, M.R. Dokmeci, A. Khademhosseini, Microfluidic techniques for development of 3D vascularized tissue, Biomaterials 35 (2014) 7308–7325, https://doi.org/10.1016/j.biomaterials.2014.04.091.
[89] M. Nguyen, A. De Ninno, A. Mencattini, F. Mermet-Meillon, G. Fornabaio, S. S. Evans, M. Cossutta, Y. Khira, W. Han, P. Sirven, F. Pelon, D. Di Giuseppe, F. R. Bertani, A. Gerardino, A. Yamada, S. Descroix, V. Soumelis, F. Mechta-Grigoriou, G. Zalcman, J. Camonis, E. Martinelli, L. Businaro, M.C. Parrini, Dissecting effects of anti-cancer drugs and cancer-associated fibroblasts by on-chip reconstitution of immunocompetent tumor microenvironments, Cell Rep. 25 (2018) 3884–3893.e3, https://doi.org/10.1016/j.celrep.2018.12.015.
[90] S.R. Nielsen, M.C. Schmid, Macrophages as key drivers of cancer progression and metastasis, Mediat. Inflamm. 2017 (2017), https://doi.org/10.1155/2017/9624760.
[91] A. Boussommier-Calleja, Y. Atiyas, K. Haase, M. Headley, C. Lewis, R.D. Kamm, The effects of monocytes on tumor cell extravasation in a 3D vascularized microfluidic model, Biomaterials 198 (2019) 180–193, https://doi.org/10.1016/j.biomaterials.2018.03.005.
[92] A. Tevlek, S. Kecili, O.S. Ozcelik, H. Kulah, H.C. Tekin, Spheroid engineering in microfluidic devices, ACS Omega 8 (2023) 3630–3649, https://doi.org/10.1021/acsomega.2c06052.
[93] N.E. Ryu, S.H. Lee, H. Park, Spheroid culture system methods and applications for mesenchymal stem cells, Cells 8 (2019) 1620, https://doi.org/10.3390/cells8121620.
[94] D.H. Ha, P.M. Thi, P. Chaudhary, J.H. Jeong, Efficient Formation of three dimensional spheroids of primary hepatocytes using micropatterned multi-well plates, Macromol. Res. 27 (2019) 938–943, https://doi.org/10.1007/s13233-019-7103-7.
[95] C. Kim, J.H. Bang, Y.E. Kim, S.H. Lee, J.Y. Kang, On-chip anticancer drug test of regular tumor spheroids formed in microwells by a distributive microchannel network, Lab Chip 12 (2012) 4135–4142, https://doi.org/10.1039/c2lc40570a.
[96] N. Dadgar, A.M. Gonzalez-Suarez, P. Fattahi, X. Hou, J.S. Weroha, A. Gaspar-Maia, G. Stybayeva, A. Revzin, A microfluidic platform for cultivating ovarian cancer spheroids and testing their responses to chemotherapies, Microsystems Nanoeng 6 (2020) 1–12, https://doi.org/10.1038/s41378-020-00201-6.
[97] J. Zhou, J. Su, X. Fu, L. Zheng, Z. Yin, Microfluidic device for primary tumor spheroid isolation, Exp. Hematol. Oncol. 6 (2017) 1–7, https://doi.org/10.1186/s40164-017-0084-3.
[98] J. Park, H. Kim, J.K. Park, Microfluidic channel-integrated hanging drop array chip operated by pushbuttons for spheroid culture and analysis, Analyst 145 (2020) 6974–6980, https://doi.org/10.1039/d0an01091j.
[99] O. Frey, P.M. Misun, D.A. Fluri, J.G. Hengstler, A. Hierlemann, Reconfigurable microfluidic hanging drop network for multi-tissue interaction and analysis, Nat. Commun. 5 (2014) 4250, https://doi.org/10.1038/ncomms5250.
[100] X. Liu, H. Lin, J. Song, T. Zhang, X. Wang, X. Huang, C. Zheng, A novel simpledrop chip for 3d spheroid formation and anti-cancer drug assay, Micromachines 12 (2021) 681, https://doi.org/10.3390/mi12060681.
[101] J.L. Teh, S.F. Abdul Rahman, G. Domnic, L. Satiyasilan, N.J.Y. Chear, D. Singh, N. Mohana-Kumaran, Rapid spheroid assays in a 3-dimensional cell culture chip, BMC Res. Notes 14 (2021) 1–6, https://doi.org/10.1186/s13104-021-05727-0.
[102] D. Vera, M. García-Díaz, N. Torras, M. Álvarez, R. Villa, E. Martinez, Engineering tissue barrier models on hydrogel microfluidic platforms, ACS Appl. Mater. Interfaces 13 (2021) 13920–13933, https://doi.org/10.1021/acsami.0c21573.
[103] C. Su, Y.J. Chuah, H.B. Ong, H.M. Tay, R. Dalan, H.W. Hou, A facile and scalable hydrogel patterning method for microfluidic 3D cell culture and spheroid-in-gel culture array, Biosensors 11 (2021) 509, https://doi.org/10.3390/bios11120509.
[104] H. Kim, C.H. Cho, J.K. Park, High-throughput culture and embedment of spheroid array using droplet contact-based spheroid transfer, Biomicrofluidics 12 (2018) 44109, https://doi.org/10.1063/1.5039965.
[105] H. Kim, H. Roh, H. Kim, J.K. Park, Droplet contact-based spheroid transfer technique as a multi-step assay tool for spheroid arrays, Lab Chip 21 (2021) 4155–4165, https://doi.org/10.1039/d1lc00581b.
[106] H. Roh, H. Kim, J.K. Park, Construction of a fibroblast-associated tumor spheroid model based on a collagen drop array chip, Biosensors 11 (2021) 506, https://doi.org/10.3390/bios11120506.
[107] D. Lee, C. Cha, The combined effects of co-culture and substrate mechanics on 3d tumor spheroid formation within microgels prepared via flow-focusing microfluidic fabrication, Pharmaceutics 10 (2018) 229, https://doi.org/10.3390/pharmaceutics10040229.
[108] A. Sargenti, F. Musmeci, F. Bacchi, C. Delprete, D.A. Cristaldi, F. Cannas, S. Bonetti, S. Pasqua, D. Gazzola, D. Costa, F. Villa, M.R. Zocchi, A. Poggi, Physical characterization of colorectal cancer spheroids and evaluation of NK cell infiltration through a flow-based analysis, Front. Immunol. 11 (2020) 564887, https://doi.org/10.3389/fimmu.2020.564887.
[109] P. Sabhachandani, V. Motwani, N. Cohen, S. Sarkar, V. Torchilin, T. Konry, Generation and functional assessment of 3D multicellular spheroids in droplet based microfluidics platform, Lab Chip 16 (2016) 497–505, https://doi.org/10.1039/c5lc01139f.
[110] P. Sabhachandani, S. Sarkar, S. Mckenney, D. Ravi, A.M. Evens, T. Konry, Microfluidic assembly of hydrogel-based immunogenic tumor spheroids for evaluation of anticancer therapies and biomarker release, J. Contr. Release 295 (2019) 21–30, https://doi.org/10.1016/j.jconrel.2018.12.010.
[111] D. Duguay, R.A. Foty, M.S. Steinberg, Cadherin-mediated cell adhesion and tissue segregation: qualitative and quantitative determinants, Dev. Biol. 253 (2003) 309–323, https://doi.org/10.1016/S0012-1606(02)00016-7.
[112] Y. Hou, Y. Zheng, X. Zheng, Y. Sun, X. Yi, Z. Wu, J.-M. Lin, Multidimensional controllable fabrication of tumor spheroids based on a microfluidic device, Lab Chip 23 (2023) 2654–2663, https://doi.org/10.1039/D3LC00251A.
[113] Q. Sun, S.H. Tan, Q. Chen, R. Ran, Y. Hui, D. Chen, C.X. Zhao, Microfluidic Formation of coculture tumor spheroids with stromal cells as a novel 3D tumor model for drug testing, ACS Biomater. Sci. Eng. 4 (2018) 4425–4433, https://doi.org/10.1021/acsbiomaterials.8b00904.
[114] M. Zoetemelk, M. Rausch, D.J. Colin, O. Dormond, P. Nowak-Sliwinska, Short-term 3D culture systems of various complexity for treatment optimization of colorectal carcinoma, Sci. Rep. 9 (2019) 1–14, https://doi.org/10.1038/s41598-019-42836-0.
[115] S.Y. Jeong, J.H. Lee, Y. Shin, S. Chung, H.J. Kuh, Co-culture of tumor spheroids and fibroblasts in a collagen matrix-incorporated microfluidic chip mimics reciprocal activation in solid tumor microenvironment, PLoS One 11 (2016) e0159013, https://doi.org/10.1371/journal.pone.0159013.
[116] J.-H. Lee, S.-K. Kim, I.A. Khawar, S.-Y. Jeong, S. Chung, H.-J. Kuh, Microfluidic co-culture of pancreatic tumor spheroids with stellate cells as a novel 3D model for investigation of stroma-mediated cell motility and drug resistance, J. Exp. Clin. Cancer Res. 37 (2018) 4, https://doi.org/10.1186/s13046-017-0654-6.
[117] S.-D. Jang, J. Song, H.-A. Kim, C.-N. Im, I.A. Khawar, J.K. Park, H.-J. Kuh, Anti-cancer activity profiling of chemotherapeutic agents in 3D co-cultures of pancreatic tumor spheroids with cancer-associated fibroblasts and macrophages, Cancers 13 (2021) 5955, https://doi.org/10.3390/cancers13235955.
[118] T. Petreus, E. Cadogan, G. Hughes, A. Smith, V. Pilla Reddy, A. Lau, M. J. O'Connor, S. Critchlow, M. Ashford, L. Oplustil O'Connor, Tumour-on-chip microfluidic platform for assessment of drug pharmacokinetics and treatment response, Commun. Biol. 4 (2021) 1–11, https://doi.org/10.1038/s42003-021-02526-y.
[119] X. Jing, F. Yang, C. Shao, K. Wei, M. Xie, H. Shen, Y. Shu, Role of hypoxia in cancer therapy by regulating the tumor microenvironment, Mol. Cancer 18 (2019) 1–15, https://doi.org/10.1186/s12943-019-1089-9.
[120] S.M. Grist, S.S. Nasseri, L. Laplatine, J.C. Schmok, D. Yao, J. Hua, L. Chrostowski, K.C. Cheung, Long-term monitoring in a microfluidic system to study tumour spheroid response to chronic and cycling hypoxia, Sci. Rep. 9 (2019) 1–13, https://doi.org/10.1038/s41598-019-54001-8.
[121] S. Gopal, S.-J. Kwon, B. Ku, D.W. Lee, J. Kim, J.S. Dordick, 3D tumor spheroid microarray for high-throughput, high-content natural killer cell-mediated cytotoxicity, Commun. Biol. 4 (2021) 893, https://doi.org/10.1038/s42003-021-02417-2.
[122] Y. Imamura, T. Mukohara, Y. Shimono, Y. Funakoshi, N. Chayahara, M. Toyoda, N. Kiyota, S. Takao, S. Kono, T. Nakatsura, H. Minami, Comparison of 2D- and 3D-culture models as drug-testing platforms in breast cancer, Oncol. Rep 33 (2015) 1837–1843, https://doi.org/10.3892/or.2015.3767.
[123] M. Ravi, A. Ramesh, A. Pattabhi, Contributions of 3D cell cultures for cancer research, J. Cell. Physiol. 232 (2017) 2679–2697, https://doi.org/10.1002/jcp.25664.
[124] K. Klimkiewicz, K. Weglarczyk, G. Collet, M. Paprocka, A. Guichard, M. Sarna, A. Jozkowicz, J. Dulak, T. Sarna, C. Grillon, C. Kieda, A 3D model of tumour angiogenic microenvironment to monitor hypoxia effects on cell interactions and cancer stem cell selection, Cancer Lett. 396 (2017) 10–20, https://doi.org/10.1016/j.canlet.2017.03.006.
[125] O. Oudar, Spheroids: relation between tumour and endothelial cells, Crit. Rev. Oncol. Hematol. 36 (2000) 99–106, https://doi.org/10.1016/S1040-8428(00)00080-9.
[126] S.M. Ehsan, K.M. Welch-Reardon, M.L. Waterman, C.C.W. Hughes, S.C. George, A three-dimensional in vitro model of tumor cell intravasation, Integr. Biol. 6 (2014) 603–610, https://doi.org/10.1039/c3ib40170g.
[127] N. Timmins, S. Dietmair, L. Nielsen, Hanging-drop multicellular spheroids as a model of tumour angiogenesis, Angiogenesis 7 (2004) 97–103, https://doi.org/10.1007/s10456-004-8911-7.
[128] J. Ahn, D.H. Kim, D.J. Koo, J. Lim, T.E. Park, J. Lee, J. Ko, S. Kim, M. Kim, K. S. Kang, D.H. Min, S.Y. Kim, Y.T. Kim, N.L. Jeon, 3D microengineered vascularized tumor spheroids for drug delivery and efficacy testing, Acta Biomater. 165 (2023) 153–167, https://doi.org/10.1016/j.actbio.2022.10.009.
[129] D. Kim, K.S. Hwang, E.U. Seo, S. Seo, B.C. Lee, N. Choi, J. Choi, H.N. Kim, Vascularized lung cancer model for evaluating the promoted transport of anticancer drugs and immune cells in an engineered tumor microenvironment, Adv. Healthc. Mater. 11 (2022) 2102581, https://doi.org/10.1002/adhm.202102581.
[130] S. Kim, H. Lee, M. Chung, N.L. Jeon, Engineering of functional, perfusable 3D microvascular networks on a chip, Lab Chip 13 (2013) 1489–1500, https://doi.org/10.1039/c3lc41320a.

[131] J. Kim, M. Chung, S. Kim, D.H. Jo, J.H. Kim, N.L. Jeon, Engineering of a biomimetic pericyte-covered 3D microvascular network, PLoS One 10 (2015) e0133880, https://doi.org/10.1371/journal.pone.0133880.
[132] M. Campisi, Y. Shin, T. Osaki, C. Hajal, V. Chiono, R.D. Kamm, 3D self-organized microvascular model of the human blood-brain barrier with endothelial cells, pericytes and astrocytes, Biomaterials 180 (2018) 117–129, https://doi.org/10.1016/j.biomaterials.2018.07.014.
[133] Y. Kameda, S. Chuaychob, M. Tanaka, Y. Liu, R. Okada, K. Fujimoto, T. Nakamura, R. Yokokawa, Three-dimensional tissue model in direct contact with an on-chip vascular bed enabled by removable membranes, Lab Chip 22 (2022) 641–651, https://doi.org/10.1039/d1lc00751c.
[134] K. Haase, G.S. Offeddu, M.R. Gillrie, R.D. Kamm, Endothelial regulation of drug transport in a 3D vascularized tumor model, Adv. Funct. Mater. 30 (2020) 2002444, https://doi.org/10.1002/adfm.202002444.
[135] K. Haase, M.R. Gillrie, C. Hajal, R.D. Kamm, Pericytes contribute to dysfunction in a human 3D model of placental microvasculature through VEGF-ang-tie2 signaling, Adv. Sci. 6 (2019) 1900878, https://doi.org/10.1002/advs.201900878.
[136] G.S. Offeddu, K. Haase, M.R. Gillrie, R. Li, O. Morozova, D. Hickman, C. G. Knutson, R.D. Kamm, An on-chip model of protein paracellular and transcellular permeability in the microcirculation, Biomaterials 212 (2019) 115–125, https://doi.org/10.1016/j.biomaterials.2019.05.022.
[137] S. Park, T.H. Kim, S.H. Kim, S. You, Y. Jung, Three-dimensional vascularized lung cancer-on-a-chip with lung extracellular matrix hydrogels for in vitro screening, Cancers 13 (2021) 3930, https://doi.org/10.3390/cancers13163930.
[138] Z. Hu, Y. Cao, E.A. Galan, L. Hao, H. Zhao, J. Tang, G. Sang, H. Wang, B. Xu, S. Ma, Vascularized tumor spheroid-on-a-chip model verifies synergistic vasoprotective and chemotherapeutic effects, ACS Biomater. Sci. Eng. 8 (2022), 1215−1225, doi: 10.1021/acsbiomaterials.1c01099.
[139] S. Koyama, S. Matsunaga, M. Imanishi, Y. Maekawa, H. Kitano, H. Takeuchi, S. Tomita, Tumour blood vessel normalisation by prolyl hydroxylase inhibitor repaired sensitivity to chemotherapy in a tumour mouse model, Sci. Rep. 7 (2017) 1–11, https://doi.org/10.1038/srep45621.
[140] E.M. Dehne, J. Hickman, M. Shuler, Biologically-inspired microphysiological systems, in: M. Balls, R. Combes, A.B.T.-T.H. Of A.T.M, in: T. Worth (Ed.), Hist. Altern. Test Methods Toxicol., Academic Press, 2018, pp. 279–285, https://doi.org/10.1016/B978-0-12-813697-3.00030-5.
[141] A. Zuchowska, S. Skorupska, Multi-organ-on-chip Approach in Cancer Research, Organs-On-A-Chip, 2022 100014, https://doi.org/10.1016/j.ooc.2021.100014, 4.
[142] A. Skardal, M. Devarasetty, S. Forsythe, A. Atala, S. Soker, A reductionist metastasis-on-a-chip platform for in vitro tumor progression modeling and drug screening, Biotechnol. Bioeng. 113 (2016) 2020–2032, https://doi.org/10.1002/bit.25950.
[143] J. Aleman, A. Skardal, A multi-site metastasis-on-a-chip microphysiological system for assessing metastatic preference of cancer cells, Biotechnol. Bioeng. 116 (2019) 936–944, https://doi.org/10.1002/bit.26871.
[144] Z. Xu, E. Li, Z. Guo, R. Yu, H. Hao, Y. Xu, Z. Sun, X. Li, J. Lyu, Q. Wang, Design and construction of a multi-organ microfluidic chip mimicking the in vivo microenvironment of lung cancer metastasis, ACS Appl. Mater. Interfaces 8 (2016) 25840–25847, https://doi.org/10.1021/acsami.6b08746.
[145] J. Hübner, M. Raschke, I. Rütschle, S. Gräßle, T. Hasenberg, K. Schirrmann, A. Lorenz, S. Schnurre, R. Lauster, I. Maschmeyer, T. Steger-Hartmann, U. Marx, Simultaneous evaluation of anti-EGFR-induced tumour and adverse skin effects in a microfluidic human 3D co-culture model, Sci. Rep. 8 (2018) 15010, https://doi.org/10.1038/s41598-018-33462-3.
[146] K.I. Kamei, Y. Kato, Y. Hirai, S. Ito, J. Satoh, A. Oka, T. Tsuchiya, Y. Chen, O. Tabata, Integrated heart/cancer on a chip to reproduce the side effects of anti-cancer drugs: in vitro, RSC Adv. 7 (2017) 36777–36786, https://doi.org/10.1039/c7ra07716e.
[147] P. Soltantabar, E.L. Calubaquib, E. Mostafavi, A. Ghazavi, M.C. Stefan, Heart/liver-on-a-chip as a model for the evaluation of cardiotoxicity induced by chemotherapies, Organs-on-a-Chip 3 (2021) 100008, https://doi.org/10.1016/j.ooc.2021.100008.
[148] A. Fedi, C. Vitale, M. Fato, S. Scaglione, A human ovarian tumor & liver organ-on-chip for simultaneous and more predictive toxo-efficacy assays, Bioengineering 10 (2023) 270, https://doi.org/10.3390/bioengineering10020270.
[149] T. Satoh, S. Sugiura, K. Shin, R. Onuki-Nagasaki, S. Ishida, K. Kikuchi, M. Kakiki, T. Kanamori, A multi-throughput multi-organ-on-a-chip system on a plate formatted pneumatic pressure-driven medium circulation platform, Lab Chip 18 (2018) 115–125, https://doi.org/10.1039/c7lc00952f.
[150] L.J.Y. Ong, T. Ching, L.H. Chong, S. Arora, H. Li, M. Hashimoto, R. DasGupta, P. K. Yuen, Y.-C. Toh, Self-aligning Tetris-Like (TILE) modular microfluidic platform for mimicking multi-organ interactions, Lab. Chip 19 (2019) 2178–2191, https://doi.org/10.1039/C9LC00160C.
[151] M. Jie, S. Mao, H. Liu, Z. He, H.F. Li, J.M. Lin, Evaluation of drug combination for glioblastoma based on an intestine-liver metabolic model on microchip, Analyst 142 (2017) 3629–3638, https://doi.org/10.1039/c7an00453b.
[152] H. Kimura, T. Ikeda, H. Nakayama, Y. Sakai, T. Fujii, An on-chip small intestine–liver model for pharmacokinetic studies, J. Lab. Autom. 20 (2015) 265–273, https://doi.org/10.1177/2211068214557812.
[153] K. Shinha, W. Nihei, T. Ono, R. Nakazato, H. Kimura, A pharmacokinetic-pharmacodynamic model based on multi-organ-on-a-chip for drug-drug interaction studies, Biomicrofluidics 14 (2020), https://doi.org/10.1063/5.0011545.
[154] P.-J.H. Zushin, S. Mukherjee, J.C. Wu, FDA Modernization Act 2.0: transitioning beyond animal models with human cells, organoids, and AI/ML-based approaches, J. Clin. Invest. 133 (2023) e175824, https://doi.org/10.1172/JCI175824.